# Sinomacrops bondei, a new anurognathid pterosaur from the Jurassic Tiaojishan Formation (China) and a new phylogenetic hypothesis for the group (#53890)

First submission

# Guidance from your Editor

Please submit by 6 Nov 2020 for the benefit of the authors (and your \$200 publishing discount).



### **Structure and Criteria**

Please read the 'Structure and Criteria' page for general guidance.



### **Custom checks**

Make sure you include the custom checks shown below, in your review.



#### **Author notes**

Have you read the author notes on the guidance page?



#### Raw data check

Review the raw data.



## **Image check**

Check that figures and images have not been inappropriately manipulated.

Privacy reminder: If uploading an annotated PDF, remove identifiable information to remain anonymous.

### **Files**

Download and review all files from the <u>materials page</u>.

- 11 Figure file(s)
- 1 Table file(s)
- 1 Raw data file(s)



### **New species checks**

- Have you checked our <u>new species policies</u>?
- Do you agree that it is a new species?
- Is it correctly described e.g. meets ICZN standard?

# Structure and Criteria



# Structure your review

The review form is divided into 5 sections. Please consider these when composing your review:

- 1. BASIC REPORTING
- 2. EXPERIMENTAL DESIGN
- 3. VALIDITY OF THE FINDINGS
- 4. General comments
- 5. Confidential notes to the editor
- Prou can also annotate this PDF and upload it as part of your review

When ready <u>submit online</u>.

## **Editorial Criteria**

Use these criteria points to structure your review. The full detailed editorial criteria is on your guidance page.

#### **BASIC REPORTING**

- Clear, unambiguous, professional English language used throughout.
- Intro & background to show context.
  Literature well referenced & relevant.
- Structure conforms to <u>PeerJ standards</u>, discipline norm, or improved for clarity.
- Figures are relevant, high quality, well labelled & described.
- Raw data supplied (see <u>PeerJ policy</u>).

#### EXPERIMENTAL DESIGN

- Original primary research within Scope of the journal.
- Research question well defined, relevant & meaningful. It is stated how the research fills an identified knowledge gap.
- Rigorous investigation performed to a high technical & ethical standard.
- Methods described with sufficient detail & information to replicate.

### **VALIDITY OF THE FINDINGS**

- Impact and novelty not assessed.
  Negative/inconclusive results accepted.
  Meaningful replication encouraged where rationale & benefit to literature is clearly stated.
- All underlying data have been provided; they are robust, statistically sound, & controlled.
- Speculation is welcome, but should be identified as such.
- Conclusions are well stated, linked to original research question & limited to supporting results.

# Standout reviewing tips



The best reviewers use these techniques

Τ	p

# Support criticisms with evidence from the text or from other sources

# Give specific suggestions on how to improve the manuscript

# Comment on language and grammar issues

# Organize by importance of the issues, and number your points

# Please provide constructive criticism, and avoid personal opinions

Comment on strengths (as well as weaknesses) of the manuscript

# **Example**

Smith et al (J of Methodology, 2005, V3, pp 123) have shown that the analysis you use in Lines 241-250 is not the most appropriate for this situation. Please explain why you used this method.

Your introduction needs more detail. I suggest that you improve the description at lines 57-86 to provide more justification for your study (specifically, you should expand upon the knowledge gap being filled).

The English language should be improved to ensure that an international audience can clearly understand your text. Some examples where the language could be improved include lines 23, 77, 121, 128 - the current phrasing makes comprehension difficult.

- 1. Your most important issue
- 2. The next most important item
- 3. ...
- 4. The least important points

I thank you for providing the raw data, however your supplemental files need more descriptive metadata identifiers to be useful to future readers. Although your results are compelling, the data analysis should be improved in the following ways: AA, BB, CC

I commend the authors for their extensive data set, compiled over many years of detailed fieldwork. In addition, the manuscript is clearly written in professional, unambiguous language. If there is a weakness, it is in the statistical analysis (as I have noted above) which should be improved upon before Acceptance.



# Sinomacrops bondei, a new anurognathid pterosaur from the Jurassic Tiaojishan Formation (China) and a new phylogenetic hypothesis for the group

 $\textbf{Xuefang Wei} \ ^{\text{Equal first author, 1, 2, 3}}, \ \textbf{Rodrigo V Pêgas} \ ^{\text{Equal first author, 4}}, \ \textbf{Caizhi Shen} \ ^{5}, \ \textbf{Yanfang Guo} \ ^{5}, \ \textbf{Waisum Ma} \ ^{6}, \ \textbf{Deyu Sun} \ ^{7}, \ \textbf{Xuanyu Zhou} \ ^{\text{Corresp. 8, 9}}$ 

Corresponding Author: Xuanyu Zhou Email address: xyzhou@elms.hokudai.ac.jp

Anurognathids are an elusive group of diminutive, potentially scansorial/arboreal pterosaurs. Even though their monophyly has been well-supported, their intrarelationships have been obscure, and their phylogenetic placement even more. In the present work, we present a new genus and species from the Middle-Late Jurassic Tiaojishan Formation, the third nominal anurognathid species from this deposit. The new species provides new information concerning morphological diversity for the group, and displays the first anurognathid skull exposed in lateral view. Furthermore, we provide a critical review of the group's phylogeny, incorporating into a single data set characters from diverging phylogenetic proposals. As a result, we obtain a new hypothesis for the placement of the group, somewhat intermediate between other two recent proposals.

<sup>1</sup> Key Laboratory of Stratigraphy and Palaeontology, Ministry of Natural Resource, Institute of Geology, Chinese Academy of Geological Sciences, Beijing,

<sup>&</sup>lt;sup>2</sup> China University of Geosciences, Beijing, China

<sup>&</sup>lt;sup>3</sup> Centre of Cores and Samples of Nature Resources, China Geological Survey, Beijing, China

Federal University of ABC, São Bernardo, Brazil

Dalian Natural History Museum, Dalian, Liaoning, China

<sup>6</sup> School of Geography, Earth and Environmental Sciences, University of Birmingham, Birmingham, United Kingdom

<sup>7</sup> Iinzhou Paleontology Museum, Jinzhou, Liaoning, China

<sup>&</sup>lt;sup>8</sup> Department of Natural History Sciences, Hokkaido University, Sapporo, Japan

<sup>9</sup> Beipiao Pterosaur Museum of China, Beipiao, Liaoning, China



# Sinomacrops bondei, a new anurognathid pterosaur

# from the Jurassic Tiaojishan Formation (China) and a

# 3 new phylogenetic hypothesis for the group

- 4 Xuefang Wei<sup>1,2,3</sup>, Rodrigo V. Pêgas<sup>4</sup>, Caizhi Shen<sup>5</sup>, Yanfang Guo<sup>5</sup>, Waisum Ma<sup>6</sup>, Deyu Sun<sup>7</sup>,
- 5 Xuanyu Zhou<sup>8,9\*</sup>

6

- 7 1. Key Laboratory of Stratigraphy and Palaeontology, Ministry of Natural Resource, Institute of
- 8 Geology, Chinese Academy of Geological Sciences, Beijing, China.
- 9 2. China University of Geosciences, Beijing, China.
- 10 3. Centre of Cores and Samples of Nature Resources, China Geological Survey, Beijing, China.
- 4. Federal University of ABC, São Bernardo, Brazil.
- 12 5. Dalian Natural History Museum, Dalian, Liaoning, China.
- 6. School of Geography, Earth and Environmental Sciences, University of Birmingham,
- 14 Birmingham, United Kingdom.
- 15 7. Jinzhou Paleontology Museum, Jinzhou, Liaoning, China.
- 16 8. Department of Natural History Sciences, Hokkaido University, Sapporo, Japan.
- 17 9. Beipiao Pterosaur Museum of China, Beipiao, Liaoning, China.

18

- 19 Corresponding Author:
- 20 Xuanyu Zhou
- 21 Email address: xyzhou@elms.hokudai.ac.jp

22

## 23 Abstract

- Anurognathids are an elusive group of diminutive, potentially scansorial/arboreal pterosaurs.
- 25 Even though their monophyly has been well-supported, their intrarelationships have been
- obscure, and their phylogenetic placement even more. In the present work, we present a new
- 27 genus and species from the Middle-Late Jurassic Tiaojishan Formation, the third nominal
- anurognathid species from this deposit. The new species provides new information concerning
- 29 morphological diversity for the group, and displays the first anurognathid skull exposed in lateral
- view. Furthermore, we provide a critical review of the group's phylogeny, incorporating into a
- 31 single data set characters from diverging phylogenetic proposals. As a result, we obtain a new



- 32 hypothesis for the placement of the group, somewhat intermediate between other two recent
- 33 proposals.

# Introduction

- 35 Pterosaurs, a group of archosauromorph reptiles, were the first vertebrates known to conquer
- active flight, with a fossil record stretching from the Late Triassic to the K/Pg boundary
- 37 (Wellnhofer 1991, Witton 2013). The Anurognathidae are a very peculiar pterosaur group still
- 38 poorly understood and rather obscure, characterized by a unique morphology and involved in a
- 39 complex history of uncertainty about its phylogenetic affinities. Spanning from the Middle
- 40 Jurassic (Callovian) to the Early Cretaceous (Aptian), anurognathids are small-sized (from 400 to
- 41 900 mm in wingspan) and exhibit short skulls with a diminutive preorbital region, huge orbits
- 42 and rounded jaws that are wider than long (Bennett 2007, Witton 2013). Due to their short wings
- with low aspect ratios and their peg-like teeth, these small pterosaurs have been interpreted as
- aerial insectivores (princt 2007, Witton 2008, 2013, Habib 2011), of possible arboreal habits
- 45 (Bennett 2007, Witton 2013, Lü et al. 2018).
- 46 The Anurognathidae have been defined as a node-based group, as the least inclusive clade
- 47 containing Anurognathus ammoni and Batrachognathus volans (Kellner 2003, Unwin 2003). So
- 48 far, this group comprises six nominal species, and is known by 12 specimens from Germany,
- 49 Kazakhstan, Mongolia, China and North Korea (with a putative 13<sup>th</sup> one from the USA). The
- 50 first described one was *Anurognathus ammoni*, coming from the Tithonian Solnhofen limestones
- of Bayaria (Döderlein 1923) and being represented by two specimens (Bennett 2007). It was not
- 52 until the second specimen was described that several aspects of its morphology were clarified,
- such as the broad wings, the short preorbital region and extensive orbit, the jugal overlying the
- maxilla, the vertical (or slightly anteriorly inclined) quadrate, the reduced palatal elements, and
- 55 the short tail lacking filiform processes of the zygapophyses and haemapophyses, convergent
- with pterodactyloids (Bennett 2007).
- 57 The second nominal species was *Batrachognathus volans*, described from an incomplete
- 58 skeleton including a partial skull from the Oxfordian-Kimmeridgian Karabastau Formation of
- 59 Kazakhstan (Riabinin 1948). A second specimen of *Batrachognathus volans* (Unwin et al.
- 60 2000), still awaiting a full description, possesses a long tail, with developed rod-like processes of
- 61 the haemapophyses and zygapophyses (Costa et al. 2013). With this discovery, Batrachognathus



- 62 *volans* became the first known anurognathid to exhibit a long tail with developed rod-like
- processes as typical of non-pterodactyloid pterosaurs (Costa et al. 2013).
- The third anurognathid to be described was *Dendrorhynchoides curvidentatus*, the first recovered
- 65 from a Cretaceous deposit, the early Aptian Jianshangou beds of the Yixian Formation (Ji & Ji
- 66 1998). Originally thought of as Barremian, these beds are now viewed as early Aptian in age (see
- 67 Chang et al. 2009). Jeholopterus ningchengensis, based on an almost complete skeleton with
- 68 extensive soft tissue preservation, was later described as another Cretaceous anurognathid (Wang
- 69 et al. 2002), on the basis of the now outdated view of the Daouhugou beds as part of the Yixian
- 70 Formation (Barremian-Aptian). Presently, these beds are interpreted as part of the Tiaojishan
- 71 Formation and dated as Callovian-Oxfordian (Liu et al. 2006, Gao & Shubin 2012). A second
- 72 specimen from the same locality has been regarded as most likely conspecific with *Jeholopterus*
- 73 *ningchengensis*, though a detailed description and a formal taxonomic assessment have not been
- provided yet (Ji & Yuan 2002, Witton 2013, Yang et al. 2019). Later, a second species for the
- 75 genus *Dendrorhynchoides*, named *D. mutoudengensis*, was erected based on an almost complete
- skeleton from the Mutoudeng locality, Tiaojishan Formation (Lü & Hone 2012). Recently, a new
- genus has been erected to accommodate this species: *Luopterus*, named after the late Prof.
- 78 Junchang Lü (Hone 2020). Moreover, a second Cretaceous anurognathid was also named
- 79 recently, Vesperopterylus lamadongensis, known from an almost complete holotype from the
- 80 late Aptian Jiufotang Formation (Lü *et al.* 2018).
- 81 Indeterminate specimens include IVPP V16728, which stands out as the second specimen with a
- 82 long tail and developed rod-like processes, similar to *Batrachognathus volans* (see Costa *et al.*
- 83 2013) and unlike all remaining anurognathids. NJU–57003 is another long-tailed specimen from
- 84 the Mutoudeng locality (Daohugou Beds, Tiaojishan Formation), only preliminarily described
- 85 (Yang et al. 2019). A relatively complete specimen from the Early Cretaceous of North Korea
- also awaits description (Gao et al. 2009), as well as a fragmentary specimen comprised of wing
- 87 elements from the Middle Jurassic (Aalenian/Bajocian) Bakhar deposits of Central Mongolia
- 88 (Bakhurina & Unwin 1995). Finally, the poorly-known *Mesadactylus ornithosphyos*, based on
- 89 the holotype BYU 2024 (a synsacrum) from the Kimmeridgian-Tithonian Morrison Formation of
- 90 the USA (Jensen & Padian 1989), is a potential anurognathid (see Bennett 2007).



91	Pterosaur phylogeny is intricated with controversies, but no other group compares to the
92	Anurognathidae when it comes to uncertainty concerning its placement (Young 1964, Kellner
93	2003, Unwin 2003, Andres et al. 2010, Dalla Vecchia 2014, 2019). Five cladistic hypotheses
94	have been presented for the phylogenetic position of the Anurognathidae, wherein they are
95	viewed as: the basalmost pterosaur group (Kellner, 2003); the sister-group of the Novialoidea
96	(Unwin, 2003); the sister-group of the Breviquartossa (Dalla Vecchia, 2019); scaphognathids,
97	whereby these are the sister-group of the Monofenestrata (Vidovic & Martill, 2018); or the
98	sister-group of the Pterodactyloidea (Andres et al., 2010; 2014). And even though the
99	monophyly of the Anurognathidae has been strongly corroborated (Kellner 2003, Unwin 2003,
100	Bennett 2007, Andres et al. 2010, Dalla Vecchia 2019), its intrarelationships have been poorly
101	explored.
102	This work presents a new fossil coming from the Mutoudeng locality, JZMP-2107500095,
103	representing a new genus and species of long-tailed anurognathid. Despit
104	obliterating some details, the specimen is rather complete and provides new information for the
105	group, including the first record of an anurognathid skull exposed in lateral view. We further
106	review the phylogenetic relationships of the group (both intra and inter), presenting an analysis
107	including all proposed species and a new hypothesis for the placement of the group.
108	
109	Geological setting
110	The Tiaojishan Formation takes its name from the Tiaojishan Mountain (Mentougou District,
111	Beijing), and was named by Ye (1920). This and the Haifanggou/Jiulongshan Formation have
112	yielded the famous Yanliao Biota in western Liaoning and adjacent regions (Huang, 2015, 2016).
113	This biota is well known for the beautiful preservation and the abundancy of insects and
114	vertebrate fossils, such as salamanders, feathered dinosaurs, pterosaurs and mammals (Sullivan
115	et al., 2014). The most important localities are Daohugou in Ningcheng County of southeast
116	Inner Mongolia, Linglongta of Jianchang County of western Liaoning Province, and Mutoudeng
117	of Qinglong County of northern Hebei Province (Lü et al. 2013). From the slightly older
118	Haifanggou Formation at Daohugou (Liu et al. 2012), pterosaurs are relatively rare, with
119	Jeholopterus ningchengensis, Pterorhynchus wellnhoferi and Daohugoupterus delicatus (Wang
120	et al. 2002, Czerkas & Ji 2002, Cheng et al. 2015). From the Tiaojishan Formation at the



121	Linglongta locality, pterosaurs are abundant in number and in diversity, wukongopterids,
122	Jianchangopterus, Jianchangnathus and Fenghuangopterus, (Wang et al. 2009, 2010; Lü et al.
123	2010, 2011a,b, Lü & Bo 2011, Sullivan et al. 2014, Cheng et al. 2012, 2016, 2017a, 2017b).
124	From the Tiaojishan Formation at Mutoudeng come <i>Dendrorhynchoides mutoudengensis</i> ,
125	Qinglongpterus guoi and Changchengopterus pani (Lü 2009, Lü et al. 2012, Lü & Hone 2012).
126	It is from the Mutoudeng locality that the new specimen herein described comes (Fig. 1).
127	The Tiaojishan Formation is mainly distributed in the Chengde Basin (Maoniujiao-
128	Xiaoguozhangzi-Jiyuqing Area) in northern Hebei Province. It is mainly composed of neutral
129	volcanic rock (Zhang & Chen, 2015). The lithology of lower member includes dark grey, grey
130	purple trachyandesites, quartz trachyandesites, small trachyandesitic agglomerate, small
131	trachyandesitic ignimbrite (Zhang & Chen, 2015). The lithology of upper member includes dark
132	grey, burgundy trachyandesites, trachyandesitic agglomerate, partially containing grayish purple
133	grayish green sedimentary tuff, tuffaceous conglomerate and tuffaceous sandstone (Zhang &
134	Chen, 2015).
135	Zhang et al. (2008) analyzed samples of volcanic rock from several typical localities (Luanping
136	Basin, Chengde Basin, Sanshijiazi Basin and Jinlingsi-Yangshan Basin), utilizing LA-ICP-MS
137	Zircon U-Pb. Their result suggest that the lower limit age of the Tiaojishan Formation should be
138	around 165 Ma. Li et al. (2019) analyzed samples of volcanic rock the bottom of the lower
139	section and andesite at the top of the upper section, utilizing LA-ICP-MS Zircon U-Pb. Their
140	result gave an age range 170-153 Ma for the Formation as a whole, that is, from the Bajocian
141	until the Kimmeridgian. A specific dating for the strata of the Linglongta locality has been
142	provided by Liu et al. (2012), in order to provide a constrained age range for wukongopterid
143	pterosaurs. The bottom and the top of this locality were dated, resulting in an age range of 161-
144	160 Ma (Liu et al., 2012), falling within the Oxfordian (early Late Jurassic). Specific dating
145	under geochemical approaches still lack for the Mutoudeng locality. However, biostratigraphic
146	studies, based mainly on conchostracans, suggest that the Linlongta and Mutoudeng strata are
147	chronocorrelate (Chu et al., 2016).

148

# **Material & Methods**



### **Institutional abbreviations** 150 **IVPP**, Institute of Vertebrate Paleontology and Paleoanthropology, Beijing, China; **JPM**, JZMP, 151 Jinzhou Museum of Paleontology, Jinzhou; NJU, Nanjing University, Nanjing, Chir 152 153 154 Computed tomography (CT) scanning JPM-2012-001 was computed tomography (CT) scanned using a Nikon XTH225ST scanner at 155 the Laboratory of Stratigraphy and Paleontology, Institute of Geology, Chinese Academy of 156 Geological Sciences (IG-CAGS), Beijing, China. The specimen was scanned at 160 kV and 131 157 μA. The data set includes 2000 image slices (2000 x 2000 pixels) with a slice thickness of 0.121 158 mm. The data was imported into digital visualization software Avizo (version 9.1) for image 159 160 processing and visualization. 161 **Phylogenetic Analysis** 162 We have performed a phylogenetic analysis based on a data matrix modified from Dalla Vecchia 163 (2019), which is focused on non-pterodactyloid relationships (see Supplementary Information for 164 our character list and coding). To this matrix, we have added the herein described species, as 165 well as Vesperopterylus lamadongensis, and have split Dalla Vecchia's (2019) OTU 166 "Dendrorhynchoides spp." into Dendrorhynchoides mutoudengensis and Luopterus 167 *curvidentatus*, coding them separately. 168 To the character list, we have added some characters from the analyses of Kellner (2003), Unwin 169 (2003) and Andres et al. (2014), as can be found in the Supplementary Material. We have further 170 added four new characters: character 7, jaws, lateral margins in dorsal or ventral view, shape (0: 171 straight or slightly concave; 1: convex and elliptical; 2: convex and semicircular); character 37, 172 orbit, size relative to skull length (0: under half of skull length; 1: half of skull length or more); 173 character 81, caudal series, length relative to femur (0: longer than 0.60 femur length; 1: equal to 174 or under 0.60 femur length); and character 115, tibia, length relative to femur (0: equal to or 175 under 1.60 tibia length; 1: over 1.60 tibia length). The TNT file with the complete data matrix is 176 available in the Supplemental Information. 177





178	The analysis was performed by TNT (Goloboff et al. 2008) using the Traditional Search option
179	with 10000 replicates (memory set at 300 MB, saving 9999 trees), random seed = 0, and
180	collapsing trees after search. All characters were treated unordered and unweighted.
181	
182	Nomenclatural acts
183	The electronic version of this article in Portable Document Format (PDF) will represent a
184	published work according to the International Commission on Zoological Nomenclature (ICZN),
185	and hence the new names contained in the electronic version are effectively published under that
186	Code from the electronic edition alone. This published work and the nomenclatural acts it
187	contains have been registered in ZooBank, the online registration system for the ICZN. The
188	ZooBank LSIDs (Life Science Identifiers) can be resolved and the associated information viewed
189	through any standard web browser by appending the LSID to the prefix http://zoobank.org/. The
190	LSID for this publication is: urn:lsid:zoobank.org:pub:15997DEB-0EF7-40F6-80B0-
191	2C40ED47D43B. LSID for the new genus: urn:lsid:zoobank.org:act:C1268C7D-80AA-4854-
192	93E7-0E60220A05BC. LSID for the new species: urn:lsid:zoobank.org:act:048E9ADE-8C3A-
193	47D4-B074-DCEFA40BDE9A. The online version of this work is archived and available from
194	the following digital repositories: PeerJ, PubMed Central and CLOCKSS.
195	
196	Results
197	Systematic Paleontology
198	Pterosauria Owen, 1842
199	Novialoidea Kellner, 2003
200	Breviquartossa Unwin, 2003
201	Monofenestrata Lü et al., 2009
202	Anurognathidae Kuhn, 1967
203	



204	Type genus. Anurognathus ammoni Döderlein, 1923.
205	<b>Definition.</b> The least inclusive clade containing <i>Anurognathus ammoni</i> and <i>Batrachognathus</i>
206	volans (Kellner 2003).
207	Synapomorphies. Skull broader than long, broadly arching jaws, skull dorsal margin convex,
208	prenarial rostrum under 20% skull length, nasoantorbital fenestra extends dorsal to premaxillary
209	tooth row, nasoantorbital fenestra higher than long, nasoantorbital fenestra anterior margin
210	bordered by premaxilla only, orbit larger than nasoantorbital fenestra, premaxillary bony bar
211	narrow, jugal anteriorly expanded overlapping maxilla laterally, quadrato-mandibular joint
212	posterior to orbit, quadrate thin and subcylindrical, jugal lacrimal process narrow, palatines
213	reduced to thin bars, unfused dentary symphysis, anterior lateral surface of dentaries pitted, iliac
214	preacetabular process straight (Kellner 2003, Unwin 2003, Andres et al. 2010, Dalla Vecchia
215	2019, this work).
216	Included species. Anurognathus ammoni, Vesperopterylus lamadongensis, Jeholopterus
217	ning chengens is,  Dendror hynchoides  curvident atus,  Luopter us  mutou dengens is,  Batrachognathus
218	volans and Sinomacrops bondei tax. nov.
219	
220	Anurognathinae Nopcsa 1928
221	<b>Definition.</b> The most inclusive clade containing <i>Anurognathus ammoni</i> but not <i>Batrachognathus</i>
222	volans (new definition).
223	Synapomorphy. Jaws semicircular in shape, pteroid curved and subparallel-sided.
224	Included species. Anurognathus ammoni, Vesperopterylus lamadongensis, Jeholopterus
225	ningchengensis, Dendrorhynchoides curvidentatus, Luopterus mutoudengensis.
226	
227	Anurognathini new clade name
228	<b>Definition.</b> The most inclusive clade containing <i>Anurognathus ammoni</i> but not <i>Luopterus</i>
229	mutoudengensis.



**Synapomorphies.** Humerus deltopectoral crest trapezoidal, tail/femur length ratio under 0.60, 230 and loss of filiform processes of the caudal zygapophyses and haemapophyses. 231 **Included species.** Anurognathus ammoni, Vesperopterylus lamadongensis and Jeholopterus 232 233 ningchengensis. 234 Batrachognathinae Kellner et al. 2010 235 **Definition.** The most inclusive clade containing *Batrachognathus volans* but not *Anurognathus* 236 ammoni (Kellner et al. 2010). 237 238 **Synapomorphies.** Humeral deltopectoral crest reduced (less wide than humeral shaft; and less wide than proximodistally long), humeral deltopectoral crest subrectangular, ulnar crest of 239 humerus rounded, humeral/femoral length ratio over 1.70, tibial/femoral length ratio over 1.60. 240 **Included species.** Batrachognathus volans and Sinomacrops bondei gen. et sp. nov. 241 242 243 Sinomacrops bondei gen. et sp. nov. **Etymology.** The generic name is a combination of *Sino*, *macro* and *ops*; which are Ancient 244 Greek for China, large, and eyes/face, respectively. This is in reference to both the large eyes and 245 the broad faces that are typical of anurognathids, and to the Chinese origin of the new species. 246 The specific epithet honors paleontologist Niels Bonde, for his many scientific contributions and 247 being an inspiration for us. 248 Holotype. JPM-2012-001 (Figs. 2–6). 249 250 Locality and horizon. Mutoudeng, Qinglong County of Hebei Province. Daohugou Beds (Callovian-Oxfordian 164-158 Ma) of the Tiaojishan Formation (see Liu et al. 2006a, 2006b, 251 Gao & Shubin 2012). 252 **Diagnosis.** The new taxon exhibits two autapomorphies: first three maxillary alveoli closely 253 spaced, and a relatively long tibia (over 1.80 times femur length). 254 255



Description

Generalities. JPM-2012-001 comprises a crushed skeleton (Fig. 2). While the cranium and some cervical vertebrae are exposed in right lateral aspect (Fig. 3), the remaining of the skeleton is exposed in ventral view. The preserved bone tissue exhibits a fragile, brittle condition. In consequence, in many regions of the skeleton, fragments of bone tissue have been lost posterior to collection of the specimen. These lost fragments left clear impressions on the matrix, indicating where they were originally present. Lost fragments include mainly the dorsal and caudal vertebrae, sternum, distal epiphysis of right humerus, proximal epiphyses of right ulna and radius, parts of the left humerus, and most of the remaining of the left wing.

Micro computed tomography scan resulted in images with only limited resolution. Nonetheless, the images permitted better visualization of some impressions on the matrix (represented by empty spaces on the slices), helping in the identification of some bone limits and extensions. Such was the case of elements of the left wing (humerus epiphysis, radius and ulna, wing metacarpal and first wing phalanx), as well as the right humerus (Fig. 4). CT images did not provide enough resolution for additional data on other skeletal regions.

- **Soft tissue.** The skeleton includes preservation of soft tissue patches. The dorsal margin of the skull is covered by skin impressions that descends onto the neck region (Fig. 3). An irregular patch of soft tissue lateral to the left tibiotarsus suggests that the brachiopatagium extended posteriorly onto the distal region of the crus. Another large patch of soft tissue is present medial to the right hindlimb, extending from the femoral region until the distal fifth of the tibiotarsus. This implies in an extensive cruropatagium, though participation of the tail in its sustenance is unclear. Deeper investigation of the soft tissue remains of JPM-2012-001 is beyond the scope of the present contribution and shall be presented elsewhere.
- Cranium. The cranium of JPM-2012-001 is exposed in right lateral aspect (Fig. 3). A small pair of bones on the rostral tip of the skull seem to represent an unfused pair of premaxillae. Individually, they comprise basically two processes, one ascending and another one extending posteriorly. This indicates that the fused premaxillae would display a T-shape similar to what is seen in *Batrachognathus volans*. The right premaxilla is exposed laterally, while the left one is slightly displaced and exposed in anteromedial aspect. The dorsal process of the premaxilla



# **PeerJ**

285	seems to have extended for no further than half the height of the skull. It contacts an anterior
286	process of the frontal, which is elongated and thin, as in <i>Anurognathus ammoni</i> (see Bennett
287	2007). The posterior process of the premaxillae participates on the occlusal jaw margin, and
288	presumably contacted the maxillae, though the bones are slightly displaced and not in natural
289	contact.
290	The maxilla and jugal are fused, with not visible sutures, forming a large bony structure,
291	posterior to the premaxillae. It forms most of the jaw as well as the ventral border of the orbit.
292	The jugo-maxilla structure houses 9 alveoli. The lacrimal process of the jugal is present on the
293	anterior region of this structure. It forms the anteroventral border of the orbit, and the
294	posteroventral margin of the nasoantorbital fenestra. It is incomplete dorsally, but is clearly
295	slender, much higher than long. The nasal and the lacrimal cannot be identified.
296	It appears that both frontals are visible: the right one in lateral aspect, and the left one in medial
297	aspect. They are both positioned on the posterodorsal region of the orbit, and take part in the
298	dorsal margin of the skull itself. Their limits are not clear, but the dorsal margin of the right
299	frontal is convex, as is the dorsal margin of the skull in lateral view. Posterior to the right frontal
300	two bones are tentatively interpreted as the right parietal and a misplaced right opisthotic.
801	A large bone bearing 9 alveoli forms most of the right upper jaw margin, and is here interpreted
302	as a jugomaxilla complex, similar to the one reported for Anurognathus ammoni where the jugal
303	overlays the maxilla laterally (Bennett 2007). The structure is seen in lateral view, and no sutures
304	can be seen separating jugal from maxilla. The right jugomaxilla seems to be disarticulated from
805	both the quadrate and the premaxilla.
306	A triangular bone located on the posterior margin of the orbit is tentatively interpreted as the
307	postorbital. If this identification is correct, then the postorbital of <i>Sinomacrops</i> is quite different
808	from that of Anurognathus, which is very slender (and dorsoventrally elongated). Thus, the
309	postorbital of <i>Sinomacrops</i> would be more similar to that of some non-anurognathid pterosaurs
310	such as <i>Dimorphodon</i> or rhamphorhynchids (e.g. Padian 1983, Wellnhofer 1991).
311	Ventral to the jugomaxilla, a rod-like bone is preserved, adjacent to the impression of another
312	similar rod-like bone. These two rod-like bones are interpreted as members of the palate, which
313	is composed of rod-like bones and bony processes (pterygoids, palatines, vomer, ectopterygoids)

# **PeerJ**

in Anurognathus ammoni, Jeholopterus ningchengensis and Batrachognathus volans (Riabini 314 1948, Bennett 2007, Yang et al. 2019). 315 A partial sclerotic ring is preserved, displaced from its natural position and located ventral to the 316 317 posterior region of the skull. Though partially preserved, it is complete enough to allow for an estimation of its diameter. It is estimated as ~7 mm, what is close to the estimated diameter of 318 the orbit (7.5 mm). 319 **Mandible.** An hemimandible is exposed beneath the skull (Fig. 3). No alveoli can be observed, 320 suggesting that it is the left hemimandible in ventral view. We infer that this hemimandible is 321 complete because its length equals that of the upper jaw. It is only slightly bowed, as in 322 Batrachognathus volans, instead of strongly semicircular as in Dendrorhynchoides 323 curvidentatus, Anurognathus ammoni or Vesperopterylus lamadongensis (Ji & Ji 1998, Bennett 324 2007, Lü et al. 2017). 325 326 **Dentition.** A single preserved tooth crown is visible, displaced from the jaws and located near 327 the anterodorsal region of the skull (Fig. 3). This tooth is slender and slightly recurved. At least 9 alveoli are present on the right maxilla. The alveoli on the right premaxilla are unclear. The first 328 three maxillary alveoli are closely spaced, with the spacing between them being shorter than 329 330 their diameter. Posteriorly, the spacing between the subsequent alveoli is subequal to their diameter. This pattern is unprecedented for anurognathids (Döderlein 1923, Riabinin 1948, Ji & 331 Ji 1998, Wang et al. 2002, Bennett 2007, Lü & Hone 2012, Lü et al. 2018, Yang et al. 2019). 332 **Axial postcranium.** Throughout the whole specimen, vertebrae are highly weathered and details 333 of their anatomy cannot be retrieved (Fig. 2). Still, as the skeleton is almost complete, the lengths 334 each segment can be estimated, with 23 mm for the cervical series; 3 mm for the dorsal series; 335 1.1 mm for the sacral series; and > 36 mm for the caudal series. The sacral series thus seems to 336 have been elongated, similarly to the condition seen in the possible anurognathid Mesadactylus 337 (see Jensen & Padian, 1989). The rib of the first sacral is strongly inclined posteriorly, while the 338 rib of the second sacral are less inclined (Fig. 5). This configuration is very similar to that of 339 Mesadactylus (see Jensen & Padian, 1989). At least 9 pairs of ribs can be seen (Fig. 2), all of 340 341 which are long and slender, and interpreted as dorsal ribs. This is the same number of dorsal ribs



Bennett 2007). 343 Forelimb. The scapulae and coracoids of JPM-2012-001 are elongate and slender, as in other 344 345 anurognathids (e.g. Bennett 2007, Lü et al. 2018). Although fragments of the bone tissue have been lost post-collection due to the brittle nature of the fossil, the remaining impression of the 346 right humerus is quite clear upon close inspection. The deltopectoral crest is subrectangular, as 347 can be better seen on the left side (Fig. 2). As in *Batrachognathus volans*, the deltopectoral crest 348 349 of the humerus in JPM-2012-001 was reduced (less wide than proximodistally long, and less wide than humeral shaft) and rectangular in shape. The shape of the ulnar crest is rounded, but it 350 is proximodistally shorter than the deltopectoral crest, as in other anurognathids (Döderlein 1923, 351 Riabinin 1948, Ji & Ji 1998, Wang et al. 2002, Bennett 2007, Lü & Hone 2012, Lü et al. 2018, 352 Yang et al. 2019). Incomplete preservation prevents the observation of any details of ulna and 353 radius, though their lengths can be assessed due to their clear impressions on both sides. The 354 right wing-finger preserves complete first, second and third wing phalanges (Fig. 2). The distal 355 region of the third wing phalanx underlies the tibia on the matrix, but the distal end can be seen 356 due to damage on the tibia, revealing the phalanx beneath. The distal end of the third wing 357 358 phalanx is slightly expanded, indicating an articular region for a four phalanx, which is not preserved. A free digit with a long, slender proximal phalanx and a robust, strongly recurved 359 ungual is preserved. 360 **Hindlimb.** Neither femora are fully preserved, though impressions of the lost regions remain on 361 both sides (Fig. 2). The left femur is preserved in an approximately natural position relative to 362 the pelvic region, and only part of the proximal region was lost, though an impression remains. 363 The right femur is displaced, but the proximal region is preserved. The distal region is lost, but 364 an impression also remains. The tibia is quite elongate relative to the femur (Fig. 2), more so 365 366 than in any other anurognathid (Table 1). On the right crus, tibia and fibula are incompletely 367 ossified, and a gap can be seen between the two (Fig. 2). Despite damage on the proximal region of the right metatarsus, the distal region is well-preserved. It can be clearly seen that the 368 metatarsal IV is shorter than metatarsals II and III (Fig. 5). A single ungual can be identified on 369 370 the right pes, which is slightly less robust than the manual unguals (Fig. 6).

seen in Dendrorhynchoides, Anurognathus, Jeholopterus (Ji & Ji 1998, Wang et al. 2002,



### Phylogenetic analysis results 372 Our analysis produced 9 most parsimonious trees, with 321 steps, CI of 0.517-0.526 and RI of 373 0.754-0.764. In the strict consensus tree (Fig. 7), the new species is the sister-group of 374 Batrachognathus volans. The Anurognathinae were recovered with Dendrorhynchoides at the 375 base, plus the newly recognized clade Luopterus + (Jeholopterus + (Anurognathus + 376 377 *Vesperopterylus*)). As in the original results from Dalla Vecchia (2019), "Dimorphodon" weintraubi is the sister-378 group of the Anurognathidae. For the first time, the clade comprising the latter two taxa is 379 recovered as the sister group of Darwinoptera + Pterodactyloidea. The synapomorphies are 380 discussed further below. 381 382 **Discussion** 383 384 Diversity of the Anurognathidae Unwin et al. (2000) and Bennett (2007) observed that some aspects of anurognathid morphology 385 did not change from the Middle Jurassic (in the form of Jeholopterus) to the Early Cretaceous (in 386 the form of *Dendrorhynchoides*; prior to the description of the even younger *Vesperopterylus*), 387 such as skull shape, palate morphology and dentition. This led these authors to consider that the 388 anurognathid bauplan was rather conservative (Unwin et al. 2000, Bennett 2007). Nonetheless, 389 several features of anurognathid morphology exhibit considerable variation, and here we show 390 that anurognathid morphological diversity is higher than previously thought. 391 Concerning the particular shape of the anurognathid jaw in dorsal/ventral views, we note that 392 there exists some variation. The roundness of the jaws (both upper and lower) is relatively more 393 pronounced in anurognathines, as can be seen particularly in *Anurognathus*, *Jeholopterus*, 394 395 Vesperopterylus and NJU-57003 (Wang et al. 2002, Ji & Yuan 2002, Bennett 2007, Lü et al. 2018, Yang et al. 2019). In these, the arching of the jaws is abrupt and approximately 396 397 continuous, describing a semicircular shape. In contrast, in *Batrachognathus* and *Sinomacrops*, the arching of the jaws is less pronounced and relatively more gradual, making the jaws rather 398 elliptical instead of semicircular (Fig. 8). 399



100	Some variation on tooth morphology is also found within anurognathids. The dentition of
101	Anurognathus ammoni is homodont and was referred to as pupiform, given their resemblance to
102	dipteran pupae (Bennett 2007). The only complete tooth preserved in the referred specimen of
103	Anurognathus ammoni is short, has a subcylindrical base and tapers to a sharp end, being only
104	slightly recurved (Bennett 2007). This is very similar to the condition seen in Vesperopterylus
105	lamadongensis, except that in this taxon the teeth are relatively stouter (see Lü et al. 2018).
106	However, the teeth in Jeholopterus ningchengensis, NJU-57003, Dendrorhynchoides
107	curvidentatus are relatively longer and more recurved. The single tooth visible in the holotype of
108	Sinomacrops bondei is superficially similar to these latter taxa. Luopterus mutoudengensis is
109	unique within anurognathids, having been described as exhibiting a heterodont dentition
10	comprising slender, sharp teeth anteriorly and relatively more robust, short teeth posteriorly (Lü
111	& Hone 2012). However, recently, Hone (2020) speculated that the purported robust teeth may
112	in fact be bone shards, although a close reinspection has not been presented yet.
113	According to Lü & Hone (2012), a noticeable amount of variation in anurognathids is also
114	expressed through the shape of the deltopectoral crest of the humerus (Fig. 9), as follows:
15	rounded for Anurognathus ammoni, alate for Jeholopterus ningchengensis, triangular for
116	Dendrorhynchoides curvidentatus and Luopterus mutoudengensis, and sub-rectangular for
17	Batrachognathus. However, in the holotype of Anurognathus, the structure is not rounded, but
118	clearly trapezoidal (Döderlein 1923, Wellnhofer 1991). Despite not clearly depicted as such in
119	the line-drawings, the humeral deltopectoral crest of the second specimen of Anurognathus was
120	also explicitly described as trapezoidal (see Bennett 2007), and is probably relatively smaller due
121	to allometric growth. In Vesperopterylus, the deltopectoral crest of the humerus is also
122	trapezoidal, very similar in shape to Anurognathus (see Lü et al. 2018). In the North Korea
123	specimen, the deltopectoral crest of the humerus seems to be trapezoidal as well (Gao et al.
124	2009). Furthermore, even though the "alate" condition seen in <i>Jeholopterus</i> is unique to it, it is
125	still very similar to the trapezoidal conditions of Anurognathus and Vesperopterylus, differing
126	only in being longer and more curved – they are thus all coded as "trapezoidal" in our analysis
127	(see Supplemental Information). Concerning other anurognathids, NJU-57003 is similar to
128	Dendrorhynchoides and Luopterus in exhibiting a subtriangular deltopectoral crest of the
129	humerus (Yang et al. 2019). In the holotype of Sinomacrops bondei, the impression of the
130	deltopectoral crest of the humerus reveals it was subrectangular in shape, being similar to that of



432 433 434	even straighter than in <i>B. volans</i> (Fig. 9A–B). <i>Sinomacrops</i> and <i>Batrachognathus</i> are further unique in exhibiting deltopectoral crests that are reduced in size, being less wide than humeral shaft, and less wide than proximodistally long (Fig. 9A–B).  Still concerning the proximal region of the humerus, considerable variation can also be found in the shape of the ulnar crest. In <i>Batrachognathus volans</i> and <i>Sinomacrops bondei</i> , the distal
	shaft, and less wide than proximodistally long (Fig. 9A–B).  Still concerning the proximal region of the humerus, considerable variation can also be found in the shape of the ulnar crest. In <i>Batrachognathus volans</i> and <i>Sinomacrops bondei</i> , the distal
434	Still concerning the proximal region of the humerus, considerable variation can also be found in the shape of the ulnar crest. In <i>Batrachognathus volans</i> and <i>Sinomacrops bondei</i> , the distal
	the shape of the ulnar crest. In Batrachognathus volans and Sinomacrops bondei, the distal
435	
436	
437	margin of the ulnar crest is rounded (Fig. 9A-B). In Dendrorhynchoides curvidentatus, it is
438	slightly more prominent, subtriangular (Fig. 9). In Jeholopterus, it is particularly reduced, and is
439	also prominent (Fig. 9D). In Anurognathus and Vesperopterylus, it is relatively elongated and
440	oriented obliquely to the humeral shaft (Fig. 9E-F).
441	Another interesting variation seen within anurognathids concerns the length of their caudal series
442	and the morphology of their caudal vertebrae (Lü & Hone 2012, Costa et al. 2013, Jiang et al.
443	2014). Batrachognathus and the indeterminate specimens IVPP V16728 and NJU-57003 exhibit
444	the typical non-pterodactyloid condition, with long tails (longer than femur length) and caudal
445	vertebrae bearing long filiform processes of the zygapohyses and haemapophyses (Costa et al.
446	2013, Jiang et al. 2014, Yang et al. 2019). Luopterus mutoudengensis exhibits a relatively short
447	caudal series, that is shorter than the dorsal series and equals 0.85 the femur length (Lü & Hone
448	2012). As for caudal vertebrae morphology, <i>Luopterus</i> was reported to bear filiform processes
449	interpreted as haemapophyses (Lü & Hone 2012). Jiang et al. (2014) have suggested that
450	Luopterus mutoudengensis possessed processes produced by both the zygapophyses and
451	haemapophyses, and we agree this is rather likely. In our matrix, the haemapophyses processes
452	are coded as present and the zygapophyses processes as "?" until a first-hand reassessment of the
453	specimen is provided. In Jeholopterus (both specimens), the tail is most likely shorter than the
454	femur, though details of vertebral morphology cannot be assessed (Wang et al. 2002, Ji & Yuan
455	2002, Jiang et al. 2014, Yang et al. 2019). Finally, Anurognathus and Vesperopterylus possess
456	quite shortened tails (accounting for under 60% the femur length) and caudal vertebrae without
457	any filiform processes, in a homoplastic condition relative to the Pterodactyloidea (see Jiang et
458	al. 2014). In Sinomacrops bondei, even though the total extent of the caudal series is uncertain,
459	the preserved impression indicates it was longer than the femur – in fact, longer than the entire
460	hindlimb.



461	
462	Intrarelationships of the Anurognathidae
463	Our phylogenetic analysis places Sinomacrops bondei alongside Batrachognathus volans
464	forming the Batrachognathinae and separately from the clade containing all other Chinese
465	anurognathids plus Anurognathus ammoni (the Anurognathinae as herein defined). Five
466	synapomorphies support Batrachognathinae in our analysis: the humeral/femoral length
467	proportion (over 1.7), the width of the humeral deltopectoral crest (reduced, less wide than
468	proximodistally long), the shape of the deltopectoral crest (subrectangular), the shape of the
469	ulnar crest of the humerus (rounded), and the tibia/femur length proportion (over 1.6).
470	The Anurognathinae are composed, according to our results, of Dendrorhynchoides
471	curvidentatus, Luopterus <mark>mutoudenensis</mark> , Jeholopterus ningchengensis, Anurognathus ammnon
472	and Vesperopterylus lamadongensis. These taxa share the semicircular arching of the jaws,
473	distinct from the elliptical one seen in batrachognathines (new character state), and the pteroid
474	shape, curved and subparallel-sided (Andres et al. 2014).
475	The non-monophyly of the genus <i>Dendrorhynchoides</i> englobing <i>D. curvidentatus</i> plus <i>D.</i>
476	mutoudengensis (Lü & Hone 2012) is corroborated here, consistently with Wu et al. (2017) and
477	Hone (2020). Luopterus mutoudengensis is recovered as the sister-group of the Anurognathini,
478	with which it shares a straight last phalanx of pedal digit V, whereas this phalanx is curved in
479	Dendrorhynchoides curvidentatus. The straight condition is a synapomorphy joining Luopterus
480	Anurognathini, while the curved condition is plesiomorphic for anurognathids and present at the
481	base of the Novialoidea, as seen in Campylognathoides, Dimorphodon weintraubi,
482	Changchengopterus pani and wukongopterids (Clark et al. 1998, Lü 2009, Padian 2008a,b,
483	Wang et al. 2009, 2010).
484	The clade composed of Jeholopterus ningchengensis, Anurognathus ammoni and
485	Vesperopterylus lamadongensis (the newly defined Anurognathini) is strongly supported by six
486	synapomorphies: deltopectoral crest of the humerus trapezoidal, caudal series shorter than 0.60
487	femur length (new character), caudal vertebrae lacking filiform zygapophyses, caudal vertebrae
488	lacking filiform haemapophyses, pedal digit V phalanx 2 straight, and pedal digit V phalanx 2
489	shorter than phalanx 1 (new character). The sister-group relationship between <i>Anurognathus</i>





490	ammoni and Vesperopterylus lamadongensis is supported by one synapomorphy: the loss of mid-
491	cervical ribs. This result is interesting in implying in the temporal coexistence, in the Tiaojishan
492	Formation, of three lineages of anurognathids: batrachognathines, Luopterus, and
493	anurognathinins.
494	Previous analyses had recovered disparate results. The results of Wang et al. (2005), derived
495	from the matrix of Kellner (2003), indicated a basal position for Anurognathus ammoni, as the
496	sister-group of a trichotomy comprising Batrachognathus volans, Jeholopterus ningchengensis
497	and Dendrorhynchoides curvidentatus, which thus composed the Batrachognathinae according to
498	this topology. The relationship between Batrachognathus volans, Jeholopterus ningchengensis
499	and Dendrorhynchoides curvidentatus was based on the following synapomorphy: a very large
500	humerus, with a humeral/femoral length proportion over 1.40 (Kellner 2003, Wang et al. 2005).
501	Such ratio (humeral/femoral length proportion) equals 1.2-1.25 for <i>Anurognathus ammoni</i> , 1.43
502	for Dendrorhynchoides curvidentatus, 1.52-1.55 for Jeholopterus ningchengensis, and 1.93 for
503	Batrachognathus volans (see Table 1). As such, it can be seen that the value for
504	Dendrorhynchoides curvidentatus and Jeholopterus are not that large, not quite close to
505	Batrachognathus but actually closer to the one found in Anurognathus. Furthermore, all
506	anurognathids that subsequently described exhibit such ratios under 1.40: Vesperopterylus
507	lamadongensis (1.35) and Luopterus mutoudengensis (1.28). Thus, all anurognathids exhibit a
508	humeral/femoral length ratio between 1.2 and 1.55, except for Sinomacrops bondei (1.80) and
509	Batrachognathus volans (1.93). In our analysis, we modified the character from Kellner (2003),
510	now considering a humeral/femoral length over 1.70.
511	This is the second phylogenetic analysis to include all known anurognathid species. The only
512	other phylogenetic analysis to have ever included all (then-known) anurognathids was the one
513	presented in the work by Wu et al. (2017), derived from Andres et al. (2014), published prior to
514	the description of Vesperopterylus lamadongensis. In this analysis, Dendrorhynchoides was not
515	recovered as monophyletic. Dendrorhynchoides curvidentatus fell at the base of the group, while
516	Luopterus mutoudengensis fell as sister-group of Batrachognathus volans. In this analysis, the
517	clade comprising all other anurognathids to the exclusion of <i>D. curvidentatus</i> was supported by
518	one synapomorphy: a fifth pedal digit phalanx 2 straight, instead of curved as in $D$ .
519	curvidentatus. This bone is clearly curved in D. curvidentatus (see Ji & Ji 1998) and straight in



520	Luopterus mutoudengensis, Anurognathus ammoni and Jeholopterus ningchengensis (Wang et
521	al. 2002, Bennett 2007, Lü & Hone 2012), however, it is unknown in Batrachognathus volans
522	(see Riabinin 1948), as well as in Sinomacrops bondei, and thus cannot join Batrachognathus
523	with the Anurognathini.
524	More recently, in the analysis of Longrich et al. (2018), also derived from Andres et al. (2014),
525	the results recovered Anurognathus ammoni as the sister-group of Jeholopterus ningchengensis,
526	with Dendrorhynchoides curvidentatus as the next successive sister-group, and then
527	Batrachognathus volans at the base of the group. Luopterus mutoudengensis was not included in
528	that analysis. Such topology is compatible with the one presented here, which differs only by the
529	inclusion of Luopterus, Vesperopterylus and Sinomacrops.
530	
531	Phylogenetic placement of the Anurognathidae
532	Previous works. The interrelationships of anurognathids have been even more obscure than their
533	intrarelationships. Five cladistic hypotheses have been put forward in the literature. In the first
534	one, the Anurognathidae have been interpreted as the basal-most known pterosaur lineage (Fig.
535	10A), as the sister-group of a clade containing all other pterosaurs (Kellner 2003, Bennett 2007,
536	Lü et al. 2018). As anurognathids span from the Callovian to the Aptian, this placement would
537	imply in an extensive ghost lineage, as the pterosaur record dates back to the Carnian-Norian
538	(see Kellner 2003). Later versions of this matrix including darwinopterans preserve the same
539	position for the Anurognathidae (e.g. Wang et al. 2009). More recent versions of this data set
540	focus solely on eupterodactyloids and do not contain a comprehensive number of non-
541	pterodactyloids (e.g. Wang et al. 2012, Holgado et al. 2019, Pêgas et al. 2019).
542	The analysis of Unwin (2003) recovered anurognathids as the sister-group of the clade
543	Campylognathoides + Breviquartossa (=Rhamphorhynchidae + Pterodactyloidea), which is
544	equivalent to the Novialoidea sensu Kellner (2003) (Fig. 10B). Recent versions of this matrix,
545	comprehending further non-pterodactyloids (including darwinopterans), preserve the same
546	position for the Anurognathidae (e.g. Codorniu et al. 2016).



547	The analyses of Dalla Vecchia (2009, 2014) recovered Anurognathidae as the sister-group of the
548	Pterodactyloidea, with <i>Rhamphorhynchus</i> as the next successive sister-group. However, these
549	analyses did not include any member of the Darwinoptera. Subsequent analyses by Britt et al.
550	(2018) and Dalla Vecchia (2019) are more comprehensive (Fig. 10C), incorporating
551	darwinopterans, and have produced a different result, with Anurognathidae + Dimorphodon
552	weintraubi being the sister-group of Rhamphorhynchidae + Monofenestrata (= Darwinoptera +
553	Pterodactyloidea), and thus within Novialoidea but outside Breviquartossa.
554	The most recent hypothesis was put forward by Vidovic & Martill (2018), whose phylogenetic
555	analysis recovered the Anurognathidae as a clade comprised within a Scaphognathidae (outside
556	Rhamphorhynchidae). Similar to the proposal of Dalla Vecchia (2014, 2019), this hypothesis
557	also places anurognathids within breviquartossans but outside the Monofenestrata.
558	Under the hypothesis first put forward by Andres et al. (2010), the Anurognathidae are
559	monofenestratans and are closer to pterodactyloids than darwinopterans and rhamphorhynchids
560	(Fig. 10D), thus being comprised within the Breviquartossa. Among all proposed hypotheses,
561	these latter two converge in recognizing a clade comprised of Rhamphorhynchidae,
562	Anurognathidae, Darwinoptera and Pterodactyloidea, though disagreeing on the relationships
563	between these four subgroups.
564	The sections below present a critical discussion of the characters behind the different hypotheses,
565	and coding differences between previous analyses and the present one. For the sake of simplicity,
566	the discussion below will follow the simplified result of our analysis: Rhamphorhynchidae +
567	(Anurognathidae + (Darwinoptera + Pterodactyloidea). We will leave <i>Dimorphodon weintraubi</i>
568	and Changchengopterus pani momentarily aside. Dimorphodon weintraubi is a species from the
569	Pliensbachian of North America, still lacking a detailed and complete description (Clark et al.
570	1998), and does not belong within the genus <i>Dimorphodon</i> (see Britt et al. 2018, Dalla Vecchia
571	2019), and thus still requires a redescription and renaming. It was recovered as the sister-group
572	of the Anurognathidae by Britt et al. (2018) and Dalla Vecchia (2019). This species and its
573	relationships with the Anurognathidae will be addressed at the end of this section.



602

603

### Anurognathids as the basalmost pterosaurs? 575 According to the analysis presented by Kellner (2003), the clade containing all other pterosaurs 576 to the exclusion of anurognathids (node B of Fig. 10A) is supported on the basis of 2 577 578 synapomorphies: (1) prenarial rostrum elongated (less than 60% of the skull length); and (2) external naris displaced posterior to premaxillary tooth row. The first feature is indeed absent in 579 580 anurognathids, due to their derived condition of an extremely shortened skull. However, the second feature is actually present in Anurognathus ammoni, Batrachognathus volans, 581 582 Jeholopterus ningchengensis (see Riabini 1948, Bennett 2007, Yang et al. 2019) and Sinomacrops bondei. 583 Node C of Fig. 10A was supported by two synapomorphies: (1) humerus less than 2.5 times but 584 more than 1.5 times longer than the metacarpal IV (1.50 < hu/mclV < 2.50); and (2) length of 585 ulna between 2 and 4 times the length of metacarpal IV (4 > ul/mclV > 2) (Kellner 2003). 586 Concerning both features, almost all pterosaurs (except for MCSNB 8950 and anurognathids) 587 exhibit them. In our analysis, both are recovered as synapomorphies for the Anurognathidae, and 588 not as simplesiomorphies. 589 Node D of Fig. 10A was supported by one synapomorphy: femur longer but less than twice the 590 591 length of metacarpal IV (Kellner 2003). The femur is about twice or longer than metacarpal IV in most anurognathids (though not in *Sinomacrops bondei*). However, in our analysis, a femur 592 about twice or longer than metacarpal IV was recovered as the plesiomorphic condition for the 593 Breviguartossa, as seen in Sordes and Scaphognathus. A femur longer but less than twice the 594 length of metacarpal IV occurs homoplastically in the Rhamphorhynchini and Pterodactyloidea + 595 Darwinoptera in our analysis. 596 Node E of Fig. 10A was supported by one synapomorphy: diameter of radius no more than half 597 that of ulna (Kellner 2003). As observed by Kellner (2003), the diameter of the radius and ulna 598 are subequal in the basal pterosaur *Preondactylus buffarini*. The same is true for its sister-group, 599 Austriadactylus cristatus (see Dalla Vecchia 2009b). The diameter of the radius is inferior to half 600

that of the ulna in *Dimorphodon*, *Campylognathoides*, *Rhamphorhynchus* and pterodactyloids

(see Kellner 2003), and was thus recovered as a synapomorphy of the clade joining them on the

analysis presented by Kellner (2003). However, the diameters of ulna and radius are subequal in



604	Changchengopterus pani and darwinopterans (then unknown in 2003), as well as Sordes and
505	Scaphognathus (rhamphorhynchids in our analysis). Thus, in our analysis, we recover that
506	subequal diameters form a synapomorphy for the Breviquartossa, reversed in Rhamphorhynchus
507	and Pterodactyloidea.
508	Finally, the clade Novialoidea (thereby named in order to encompass Campylognathus and the
509	Breviquartossa) is supported by two synapomorphies: (1) third phalanx of manual digit IV
510	shorter than first (ph3d4); and (2) third phalanx of manual digit 1V shorter than second (ph3d4).
511	Both of these two features were coded as "?" for Anurognathus ammoni, Batrachognathus
512	volans and Dendrorhynchoides curvidentatus in the data matrix of Kellner (2003). However,
513	both features are present in D. curvidentatus (see Ji & Qiang 1988, Ji & Ji 1998). Presently, these
514	features are also known to be present in Anurognathus ammoni, Jeholopterus ningchengensis,
515	Luopterus mutoudengensis and Vesperoptertylus lamadongensis (Wang et al. 2002, Bennett
516	2007, Lü & Hone 2012, Lü et al. 2018).
517	The features of the next relevant node, that of the Breviquartossa, will be discussed further
518	below. The discussion above justifies why, under the present analysis, anurognathids cannot be
519	viewed as the basalmost pterosaurs.
520	
521	Anurognathids as the sister-group of Novialoidea?
522	Moving on to the analysis presented by Unwin (2003), the clade containing Campylognathoides,
523	rhamphorhynchids and pterodactyloids (equivalent to the Novialoidea) to the exclusion of
524	anurognathids was supported on the basis of six synapomorphies: (1) rostrum low with straight
525	or concave dorsal outline; (2) posterior process of premaxillae interfingers between frontals; (3)
526	external naris low and elongate; (4) nasal process of maxilla inclined backwards; (5) broad
527	maxilla-nasal contact; (6) orbit larger than antorbital fenestra. In order to better organize the
528	discussion on these six features, the comments below are numbered.
529	Comments:



530	1.	Rostrum low with straight or concave dorsal outline.
531		The dorsal outline of the rostrum of anurognathids is indeed convex, as can be seen in
532		Anurognathus ammoni (Döderlein 1923, Bennett 2007) and Sinomacrops bondei, but it is
533		not convex in most other basal pterosaurs (see Dalla Vecchia 2014, 2019) such as
534		Austriadactylus, Preondactylus, Arcticodactylus, Carniadactylus, Raeticodactylus and
535		Eudimorphodon (contra Unwin 2003). Only in dimorphodontids is the outline convex as
536		well (Padian 1983, Britts et al. 2018), though this was recovered as a homoplasy relative
537		to anurognathids in our analysis.
538	2.	Posterior process of premaxillae interfingers between frontals.
539		A posterior process of premaxillae interfingering between the frontals is present in
540		Anurognathus, as reported by Bennett (2007).
541	3.	External naris low and elongate.
542		An external naris low and elongate is indeed absent in anurognathids (see Bennett 2007).
543	4.	Nasal process of maxilla inclined backwards – 5. Broad maxilla-nasal contact.
544		A nasal process of the maxilla, as well as a contact between maxilla and nasal, are
545		actually absent in anurognathids (see Andres et al. 2010 and discussion below).
546		Furthermore, a posteriorly inclined nasal process of the maxilla is widely distributed
547		within basal pterosaurs (and not only novialoids), as seen in Preondactylus,
648		Austriadactylus, Arcticodactylus, Carniadactylus, Seazzadactylus, Raeticodactylus,
549		Caelestiventus and Dimorphodon (Dalla Vecchia 1998, 2009, 2013, 2018, 2019, Dalla
550		Vecchia et al. 2002, Stetcher 2008, Britt et al. 2018).
551	6.	Orbit larger than antorbital fenestra.
552		An orbit larger than the antorbital fenestra is present in Campylognathoides and
553		rhamphorhynchids, thus being a synapomorphy for the node joining them according to
654		Unwin (2003). An individual antorbital fenestra is not present in anurognathids (see
655		further below), but still, the orbit in anurognathids is much larger than the nasoantorbital
656		fenestra as a whole (Bennett 2007), what actually could suggest affinities to the
657		Novialoidea.
658	Theref	ore, anurognathids cannot be confidently excluded from the Novialoidea (contra Unwin
559	2003).	Still concerning the analysis of Unwin (2003), the Breviquartossa (excluding



anurognathids) shared seven synapomorphies: (1) ventral margin of skull curved downwards posteriorly; (2) loss of "coronoid" eminence on posterior end of mandible; (3) development of bony mandibular symphysis; (4) mandibular symphysis more than 30% the length of the mandible; (5) loss of heterodonty in the mandibular dentition; (6) metacarpals I, II and III of equivalent length; and (7) a short metatarsal IV. However, five of these features actually support the placement of the Anurognathidae within the Breviquartossa. Comments are again numbered below.

### Comments:

- 1. Ventral margin of skull curved downwards posteriorly.
- A ventral margin of the skull curved downwards posteriorly was coded as absent in
  Anurognathidae by Unwin (2003), and as absent in *Anurognathus* and
  Batrachognathus by Dalla Vecchia (2019), but this feature cannot be assessed in any
  of the two known specimens of *Anurognathus* (Döderlein 1923, Bennett 2007), nor in
  the holotype of Batrachognathus (see Riabinin 1948). In our analysis, this feature was
  recoded as "?" for them. In Sinomacrops, it can be seen that the feature is present, and
  was coded as such for this new taxon.
  - Loss of "coronoid" eminence on posterior end of mandible.
     A "coronoid" eminence in the lower jaw was coded as present for the Anurognathidae by Unwin (2003), but is absent in *Anurognathus* (Bennett 2007) and cannot be assessed in other species.
  - 3. Development of bony mandibular symphysis.
    - Development of an extended mandibular symphysis is indeed absent in anurognathids, as can be seen in *Sinomacrops*, *Anurognathus*, *Batrachognathus*, *Jeholopterus* and *Vesperopterylus* (Döderlein 1923, Riabinin 1948, Wang *et al.* 2002, Lü *et al.* 2018). In our analysis, the development of an extended mandibular symphysis was once again recovered as a synapomorphy of the Breviquartossa, but its absence was recovered as a reversion for the Anurognathidae. Intuitively, we propose that the secondary loss of the symphysis extension in anurognathids is biologically related to the evolutionary process of shortening of the rostrum, a derived feature of anurognathids.



690	4.	Mandibular symphysis more than 30% the length of the mandible.
691		See above (3).
692	5.	Loss of heterodonty in the mandibular dentition.
693		The particular heterodonty of basal pterosaurs is actually absent in anurognathids (e.g.
694		Dalla Vecchia 2014, 2019, contra Unwin 2003), further corroborating their placement
695		within the Breviquartossa.
696	6.	Metacarpals I, II and III of equivalent length.
697		Similarly, metacarpals I-III are of equivalent size in anurognathids, as in other
698		breviquartossans (Ji & Ji 1998, Wang et al. 2002, Bennett 2007, Lü et al. 2018, Yang
699		et al. 2019, contra Unwin 2003).
700	7.	Short metatarsal IV.
701		Finally, a review of the configuration of the fourth metatarsal in anurognathids further
702		supports their interpretation as breviquartossans. The metatarsals of $Batrachognathus$
703		volans, Luopterus mutoudengensis and Dendrorhynchoides curvidentatus can hardly
704		be discerned (Riabinin 1948, Ji & Ji 1998, Lü & Hone 2012), and this condition was
705		thus coded as "?" for them in our analysis. However, in Sinomacrops bondei, it can be
706		clearly seen that metatarsal IV is distinctively shorter than metatarsals I-III (Fig. 5). In
707		Vesperopterylus the metatarsals are very clearly preserved, so that it can be also seen
708		that metatarsals I-III are subequal while metatarsal IV is noticeably shorter (Lü et al.
709		2018). The same is true for Jeholopterus, both the holotype (Wang et al. 2002) and
710		the referred specimen (Ji & Yuan 2002, Yang et al. 2019). Only in Anurognathus can
711		it be clearly seen that metatarsal IV is subequal to the other metatarsals (Bennett
712		2007). In our analysis, this condition for <i>Anurognathus</i> represents a reversion.
713	Therefore	, the analysis presented by Unwin (2003) cannot support exclusion of the
714	Anurogna	thidae from the Breviquartossa.
715		
716	Anurogna	athids as non-breviquartossan novialoids?
717	According	g to the analysis presented by Dalla Vecchia (2019), anurognathids are novialoids

(contra Kellner 2003, Unwin 2003), but are excluded from the Breviquartossa (Fig. 10C). Under

718



719	the analysis of Dalla Vecchia (2019), the Breviquartossa, to the exclusion of anurognathids,
720	share three synapomorphies: (1) ventral margin of skull curved downwards posteriorly; (2) the
721	development of a dentary symphysis; and (3) metatarsals tightly bounded (instead of spreading
722	as in rhamphorhynchids, darwinopterans and Pterodactylus).
723	The first and second features were already explored (see above). As for the third feature, the
724	ancestral condition for the Breviquartossa was recovered as ambiguous in our analysis. We
725	therefore question a non-breviquartossan nature for anurognathids.
726	
727	Anurognathids as "scaphognathids"?
728	In the analysis presented by Vidovic & Martill (2018), the Anurognathidae are comprised within
729	a Scaphognathidae group (Fig. 10E). Note that the Scaphognathidae sensu Vidovic & Martill
730	(2018) was recovered outside of the Rhamphorhynchidae, differently from the analysis presented
731	here, as well as from Andres et al. (2014) and Dalla Vecchia (2019), which have recovered
732	Scaphognathus, or the Scaphognathinae, as comprised within Rhamphorhynchidae. Turning back
733	to the analysis of Vidovic & Martill (2018), their Scaphognathidae was recovered as the sister-
734	group of the Monofenestrata (Fig. 10E).
735	In their analysis, monofenestratans share the following 7 features to the exclusion of
736	scaphognathids (including anurognathids): (1) greater angle of the quadrate to the occlusal
737	margin of the rostrum (transformed from 130° to 139.5°-150.5°); (2) the orbit is lower relative to
738	the skull depth; (3) orbit comparatively larger relative to the inferior temporal fenestra length; (4)
739	the center of the orbit lies above the quadrate; (5) a longer, lower nasoantorbital fenestra (6)
740	nasal contacts the antorbital fenestra; and (7) nares and antorbital fenestra is confluent.
741	Comments:
742	1. Quadrate angle.
743	This angle is low in anurognathids, in which the quadrate is approximately
744	perpendicular relative to the jawline. However, in the present analysis, this is



745		recovered as apomorphic for anurognathids. It differs not only from
746		monofenestratans, but even from Scaphognathus (135°, see Bennett 2014).
747	2.	Orbit relatively lower relative to skull depth (continuous character).
748		It is unclear what difference was found between monofenestratans and
749		scaphognathids (including anurognathids) relative to this feature. The ratio between
750		orbit height and skull height is similar across non-pterodactyloid breviquartossans, as
751		the orbit height is 66% of skull height in Dorygnathus, 54-68% in Rhamphorhynchus,
752		65% in Scaphognathus, ~69% for Darwinopterus and 64% for Kunpengopterus
753		(Wellnhofer 1975, Padian 1983, 2008a, Bennett 2007, 2014, Lü et al. 2009, Wang et
754		al. 2010). The codification in their dataset should be revised, as the values in non-
755		monofenestratan breviquartossans and darwinopterans are too similar to distinguish
756		between non-monofenestratans and monofenestratans. The value for <i>Anurognathus</i>
757		ammoni is ~71% (Döderlein, 1923) and for Sinomacrops bondei is ~75%.
758	3.	Lower nasoantorbital fenestra (continuous character).
759		This character is not much informative for anurognathids, since confidently
760		measuring the height/depth of the nasoantorbital fenestra is not feasible in any known
761		anurognathid species due to crushing. Anyway, we do agree that the nasoantorbital
762		fenestra is higher in anurognathids relative to darwinopterans + pterodactyloids,
763		which share longer, lower nasoantorbital fenestra. This feature does set anurognathids
764		apart from darwinopterans + pterodactyloids, what is consistent with the results
765		presented here.
766	4.	Orbit comparatively larger relative to the lower temporal fenestra (LTF) length
767		(continuous character).
768		However different this ratio may be between scaphognathids/scaphognathines and
769		monofenestratans according to Vidovic & Martill (2018), the extension of the LFT
770		cannot be confidently estimated in any anurognathid specimen.
771	5.	Center of the orbit lies above the quadrate.
772		Throughout non-monofenestratans, the center of the orbit typically lies anterior to the
773		level of the quadrate, as seen in Scaphognathus and anurognathids, indeed (Bennett
774		2007, 2014). However, the same is true for all wukongopterids (Lü et al. 2009, Wang
775		et al. 2009, 2010). In the dataset presented by Vidovic & Martill (2018),



777

778

779

780

781

782

783

784

785

786

787

788

789

790

791

792

793

794

795

796

797

798

799

800

801

802

803

804

805

806

wukongopterids were miscoded as exhibiting the center of the orbit above the quadrate, what led to the mistaken recovery of this feature as a purported synapomorphy of the Monofenestrata, but should be restricted to pterodactyloids (though not universal).

- 6. Nasal contacts the "antorbital fenestra". The nasal does seem to contact the remnant of the "antorbital fenestra" space in *Anurognathus ammoni* (see Bennett, 2007), as well as in *Sinomacrops bondei*, although this is hard to confirm due to the crushed nature of the available specimens. Thus, this feature cannot be considered as absent in anurognathids, and is possibly present.
- 7. Nares and antorbital fenestra are confluent.

Most workers have coded a confluent nasoantorbital fenestra as absent for anurognathids (Kellner 2003, Unwin 2003, Bennett 2007, Lü et al. 2018, Vidovi & Martill 2018), except for Andres et al. (2010; 2014) and Dalla Vecchia (2019). Due to the extremely reduced preorbital region and the small absolute size of anurognathids. investigation of their preorbital fenestration is indeed difficult. In most specimens, the situation cannot be confirmed, such as the holotypes of *Jeholopterus ningchengensis*, Dendrorhynchoides curvidentatus, Luopterus mutoudengensis and Vesperopterylus lamadongensis, and also the specimen NJU-57003. The only specimen for which a skull element could be observed and tentatively interpreted as an ascending process of the maxilla (and thus a bony bar effectively separating naris and antorbital fenestra, as two distinct openings) is the second specimen of Anurognathus ammoni (Bennett 2007). The identification of this process has been reviewed and challenged by Andres et al. (2010), who argued that the purported process could not be unequivocally identified as an ascending maxillary process separating the nares from the antorbital fenestra, as it could only be seen on the right side, was a faint impression, and was displaced, so that even its natural orientation cannot be unambiguously assessed. Based on its rough location and shape, we offer a tentative interpretation for it as a palatal element. Andres et al. (2010) further noted that there are two previously described anurognathid specimens in which the preorbital region is well preserved and the ascending processes of the maxilla is absent on both sides; the holotype of



Batrachognathus and CAGS IG 02-81 (see Riabinin 1948, Ji & Yuan 2002, Andres et 807 al. 2010, Yang et al. 2019). In accordance, in the small preorbital region of 808 Sinomacrops, only a single opening is present. We favor the interpretation of Andres 809 et al. (2010) that a nasoantorbital fenestra is present in anurognathids. 810 Furthermore, Vidovic & Martill (2018) proposed five synapomorphies that defined their 811 812 Scaphognathidae to the inclusion of anurognathids: (1) humerus slenderer than the ancestral condition (continuous character); (2) tooth crowns are recurved; (3) the displacement of tooth 813 curvature is at least one tooth width; (4) the preorbital rostrum lateral margin is convex in dorsal 814 view; and (5) the prepubic boot is spatulate and narrow. We discuss below problems related to 815 features 2–5. 816 Comments: 817 2. Tooth crowns, recurved. 818 819 This feature was recovered as a synapomorphy of scaphognathids (including 820 anurognathids) sensu Vidovic & Martill (2018). In the dataset presented by these workers, this feature was coded as "?" in Rhamphorhynchus, Dorygnathus, 821 Campylognathoides and Dimorphodon. However, this feature is not unknown in these 822 823 taxa; instead, it is well-reported as present in these forms (Wellnhofer 1975, Padian 1983, 2008a,b). As such, in the present analysis, a posteriorly recurved tooth crown, 824 character 56(0), is plesiomorphic for both anurognathids and scaphognathines. 825 3. Tooth crown curvature displacement. 826 As mentioned by Vidovic & Martill (2018), this character comes from the dataset of 827 Andres et al. (2014). Curved tooth crows whose curvature displacement is equivalent 828 829 to at least the crown diameter had already been recovered as characteristic of the Rhamphorhynchidae by Andres et al. (2014), englobing species considered as 830 scaphognathids by Vidovic & Martill (2018). However, this feature is not present in 831 anurognathids, as can be seen from the well-preserved teeth of *Anurognathus*, 832 Batrachognathus, Dendrorhynchoides and Jeholopterus (Riabinin 1948, Ji & Ji 1998, 833 Wang et al. 2002, Bennett 2007). Accordingly, in the original dataset of Andres et al. 834 (2014), this feature was not coded as present in anurognathids.

835



837

838

839

840

841

842

843

844

845

846

847

848

849

850

851

852

853

854

855

856

857

858

4.	Preorbital lateral margin convex (in dorsal view).
	In the matrix presented by Vidovic & Martill (2018), this character describes the
	shape of the preorbital rostrum in dorsal view. It is thus similar to our character 7(1)
	jaws, lateral margins in dorsal or ventral view, convex and elliptical. In our present
	analysis, character 7(1) was recovered as a homoplasy between anurognathids and
	Scaphognathus.

5. Prepubis spatulate and narrow.

This feature was included in the synapomorphy list of the Scaphognathidae sensu Vidovic & Martill (2018) in their supplementary text. However, even though this feature was indeed recovered as a synapomorphy for the Scaphognathidae sensu Vidovic & Martill (2018), this character state does not join anurognathids and scaphognathids, and is not present in anurognathids. Character 208 of Vidovic & Martill (2018), relative to prepubic "boot" shape, contains three states: rounded/rocker shaped (0); angular, square (1); angular, triangular (2); and spatulate (3). In their dataset, state 3 is entirely restricted to non-anurognathid scaphognathids (and present as well in *Rhamphorhynchus* as a homoplasy). *Jeholopterus* is coded as "0", to which we agree (Wang et al. 2002), and not as spatulate. Jeholopterus is the only anurognathid species coded for this character, and the configuration is unknown for other anurognathids. This was recovered as a reversion by Vidovic & Martill (2018). In our present analysis, this is recovered as a plesiomorphy for *Jeholopterus*, and not as a reversion. Either way, even according to the dataset of Vidovic & Martill (2018), it is safe to say that anurognathids and scaphognathids do not share a similar prepubic morphology.

859

860

861

862

863

864

### Anurognathids as the sister-group of the Pterodactyloidea?

In the analysis presented by Andres *et al.* (2014) and Longrich *et al.* (2018), anurognathids are breviquartossans. More specifically, they are recovered as monofenestratans. Within the Breviquartossa, the Monofenestrata is a synapomorphy-based clade defined by the presence of a confluent nasoantorbital fenestra synapomorphic with that in *Pterodactylus antiquus* (Lü *et al.* 



2010, Andres et al. 2014). According to the analyses of Andres et al. (2010, 2014) and Longrich 865 et al. (2018), this clade comprises anurognathids, darwinopterans and pterodactyloids, based on 866 four synapomorphies: (1) confluent nasoantorbital fenestra; (2) atlantoaxis fusion; (3) mid-867 cervical neural spines low; (4) eight cervical neural spine low. All of these features support 868 placement of the Anurognathidae within the Monofenestrata (contra Kellner 2003, Unwin 2003, 869 Dalla Vecchia 2019). 870 Comments: 871 1. Confluent nasoantorbital fenestra. 872 In our present analysis, this feature is coded as present in *Jeholopterus*, 873 Batrachognathus and Sinomacrops, as explored in the section above. 874 2. - 4. Concerning cervical morphology, atlantoaxis fusion was reported for 875 Anurognathus (see Bennett 2007) and the neural spines of the cervicals are low in 876 Vesperopterylus (see Lü et al. 2018). 877 878 Therefore, all of the comments above corroborate the monofenestratan nature of anurognathids. Within the Monofenestrata, under the work of Andres et al. (2010, 2014) and Longrich et al. 879 (2018), three synapomorphies joined the Anurognathidae and the Pterodactyloidea, to the 880 881 exclusion of darwinopterans; (1) mid-cervical ribs reduced; (2) less than 15 caudal vertebrae; (3) filiform processes of the caudal zygapophyses reduced. 882 Comments: 883 1. Mid-cervical ribs are often hard to preserve, but developed ones (though relatively 884 short) have been reported for *Jeholopterus* (see Wang et al. 2002) though seem to 885 be absent in *Anurognathus* and *Vesperopterylus* (see Bennett 2007, Lü et al. 886 2018). However, slender mid-cervical ribs are also clearly present in the 887 888 Darwinoptera (Wang et al. 2009, 2010, Cheng et al. 2017). 2. -3. Concerning the last two caudal features, they were coded as "?" for 889 Batrachognathus by Andres et al. (2010), but later works demonstrated that they 890 are both present in this taxon (Costa et al. 2013, Jiang et al. 2014), and are coded 891 as such in the present analysis. The same is true for the caudals of *Luopterus* 892





893	mutoudengensis and IVPP V16728 (Lü & Hone 2012, Jiang et al. 2014). In our
894	analysis, the diminishment of the caudal series and the loss of the filiform
895	processes of the zygapophyses and haemapophyses in Jeholopterus +
896	(Anurognathus + Vesperopterylus) were recovered as homoplastic conditions
897	relative to the Pterodactyloidea.
898	Due to the comments above, we regard that a clade joining anurognathids and
899	pterodactyloids, to the exclusion of darwinopterans, is questionable.
900	
901	Anurognathids as basal monofenestratans (new hypothesis)
902	After taking into account all of the observations above and incorporating them into the dataset of
903	Dalla Vecchia (2019), our final result provides strong support for the inclusion of the
904	Anurognathidae within the Breviquartossa (contra Kellner 2003, Unwin 2003, Dalla Vecchia
905	2019) and, more specifically, within the Monofenestrata (as in Andres et al. 2010, 2014), though
906	not closer to pterodactyloids than darwinopterans (contra Andres et al. 2010, 2014). In this way,
907	our results represent a new hypothesis for the position of the group, being somewhat
908	intermediate between the results of Andres et al. (2010) and of Dalla Vecchia (2009, 2019).
909	In our analysis, the Breviquartossa (including anurognathids) is supported by six
910	synapomorphies: (1) skull ventral margin at the articulation with mandible curving down
911	posteriorly; (2) dentary anterior end straight; (3) sternal plate lateral processes on each side of
912	posterior end absent; (4) metacarpals I-III subequal in length; (5) fibula not reaching the tarsus;
913	and (6) metatarsal IV shorter than metatarsals I-III. The Monofenestrata (including
914	anurognathids, darwinopterans and pterodactyloids) are supported by four features: (1) confluent
915	nasoantorbital fenestra present; (2) atlantoaxis fusion; (3) low mid-cervical neural spines; and (4)
916	mid-cervical ribs reduced. Finally, Darwinoptera + Pterodactyloidea is supported by four
917	features that are absent in anurognathids: (1) elongated skull (over four times skull height); (2)
918	maxillary process of the premaxilla bordering ventrally the external naris absent; (3)
919	deltopectoral crest of humerus tongue-like (sensu Unwin 2003); and (4) femur longer but less



920	than twice the length of metacarpal IV (homoplastic with Rhamphorhynchini, Eudimorphodon
921	and Carniadactylus).
922	
923	A remark on Dimorphodon weintraubi
924	This is a North American Pliensbachian taxon, represented by a partial skeleton still mostly
925	undescribed (Clark et al. 1989) and awaiting a detailed description. If D. weintraubi is taken into
926	consideration, it is recovered as the immediate sister-group of the Anurognathidae (Dalla
927	Vecchia 2009, 2014, 2019, present work). Their relationship is supported by three
928	synapomorphies: (1) first wing phalanx under 0.35 total wing digit length; (2) wing phalanx 2
929	shorter than phalanx 1; and (3) a boot-like prepubis (see Dalla Vecchia 2009, 2014, 2019). D.
930	weintraubi further exhibits a conspicuously shortened metatarsal IV (Clark et al. 1998), typical
931	of the Breviquartossa.
932	If this relationship and our new results are correct, then D. weintraubi pushes the origin of the
933	Monofenestrata back to the Early Jurassic (Pliensbachian). The Early-Middle Jurassic pterosaur
934	record is rather scanty, and the diversity of monofenestratans during that time might have been
935	higher than previously thought. Such scenario is not that farfetched, given that the sister-group of
936	the Monofenestrata, the Rhamphorhynchidae, dates back to the Toarcian. A detailed
937	redescription and reassessment of D. weintraubi is of the uttermost importance.
938	
939	Conclusions
940	JZMP-2107500095 represents a new anurognathid, here named Sinomacrops bondei (Fig. 10). It
941	is the third anurognathid from the Tiaojishan Formation, and the first anurognathid specimen to
942	exhibit a skull exposed in lateral view. In our new phylogenetic analysis, it is recovered as the
943	sister-group of Batrachognathus volans, with which it composes the Batrachognathinae. All
944	other taxa were recovered as closer to Anurognathus, composing the Anurognathinae. The
945	exclusion of Luopterus mutoudengensis from the genus Dendrorhynchoides is corroborated.



946	Vesperopterylus lamadongensis is recovered as the sister-group of Anurognathus ammoni, with
947	Jeholopterus ningchengensis as their successive sister-group.
948	Some previous interpretations of anurognathid morphology and systematics have relied on
949	limited available information. With time and new specimens being discovered, new data have
950	been provided and new interpretations were presented. For this reason, each new specimen is
951	crucial for the understanding of the group. The present information available leads us to
952	reinterpret the phylogenetic position of the Anurognathidae lineage, as the sister-group of
953	Darwinoptera + Pterodactyloidea.
954	
955	Acknowledgements
956	We thank the Willi Hennig Society for making TNT freely available. We thank Q. Fang and G.
957	Wu (IG-CAGS) for assistance in CT-scanning. Special thanks to C. Zhao for kindly providing
958	his artwork. XW and XZ thank National Natural Science Foundation of China (grant #41688103,
959	#41672019, #41790452), National Key R&D Program of China (2019YFC0605403), China
960	Geological Survey (DD20190397). RVP thanks Maria E. Leal (Aarhus University) for
961	discussions, and FAPESP for a scholarship (#2019/10231-6). XW, CS, WM and XZ thank the
962	late Junchang Lü (IG-CAGS) for his guidance and support. RVP and XZ deeply thank Niels
963	Bonde (Zoological Museum, Copenhagen) for his heartful support and for fostering our
964	productive network.
965	
966	References
967	Andres, B., Clark, J. M., and Xing, X. 2010. A new rhamphorhynchid pterosaur from the
968	Upper Jurassic of Xinjiang, China, and the phylogenetic relationships of basal
969	pterosaurs. Journal of Vertebrate Paleontology, 30 (1), 163–187.
970	Andres, B., Clark, J.M. and Xu, X. 2014. The earliest pterodactyloid and the origin of the
971	group. Current Biology, 24, 1011–1016.



- 972 Bakhurina, N. N., and Unwin, D. M. 1995. A survey of pterosaurs from the Jurassic and
- 273 Cretaceous of the former Soviet Union and Mongolia. *Historical Biology* **10**, 197–245.
- 974 Bennett, S. C. 2007. A second specimen of the pterosaur Anurognathus
- 975 ammoni. Paläontologische Zeitschrift, **81** (4), 376.
- 976 **Bennett, S. C. 2014.** A new specimen of the pterosaur *Scaphognathus crassirostris*, with
- omments on constraint of cervical vertebrae number in pterosaurs. *Neues Jahrbuch für*
- 978 *Geologie und Paläontologie-Abhandlungen*, **271** (3), 327-348.
- 979 Britt, B. B., Dalla Vecchia, F. M., Chure, D. J., Engelmann, G. F., Whiting, M. F., and
- Scheetz, R. D. 2018. Caelestiventus hanseni gen. et sp. nov. extends the desert–dwelling
- pterosaur record back 65 million years. *Nature ecology and evolution*, **2** (9), 1386–1392.
- 982 Clark, J. M., Hopson, J. A., Fastovsky, D. E., and Montellano, M. 1998. Foot posture in a
- 983 primitive pterosaur. *Nature*, **391** (6670), 886–889.
- 984 Codorniú, L., Carabajal, A. P., Pol, D., Unwin, D. M. and Rauhut, O. W. 2016. A Jurassic
- pterosaur from Patagonia and the origin of the pterodactyloid neurocranium. *PeerJ*, 4, e2311.
- 986 Costa, F. R., Alifanov, V., Dalla Vecchia, F. M., Kellner, A. W. A. 2013. On the presence of
- an elongated tail in an undescribed specimen of *Batrachognathus volans* (Pterosauria:
- Anurognathidae: Batrachognathinae). *In* Sayão, J. M., Costa, F. R., Bantim, R. A. M.,
- Kellner, A. W. A. (eds). Short communications, Rio Ptero 2013 International Symposium on
- 990 *Pterosaurs*. Rio de Janeiro: Universidade Federal do Rio de Janeiro, Museu Nacional, 54–56.
- 991 Chang, S. C., Zhang, H., Renne, P. R., and Fang, Y. 2009. High-precision 40Ar/39Ar age for
- the Jehol Biota. *Palaeogeography, Palaeoclimatology, Palaeoecology*, **280** (1–2), 94–104.
- 993 Cheng, X., Wang, X., Jiang, S., & Kellner, A. W. 2012. A new scaphognathid pterosaur from
- western Liaoning, China. *Historical Biology*, **24** (1), 101-111.
- 995 Cheng, X., Wang, X., Jiang, S., Kellner, A. W. 2015. Short note on a non-pterodactyloid
- pterosaur from Upper Jurassic deposits of Inner Mongolia, China. *Historical Biology*, **27** (6),
- 997 749-754.



- 998 Cheng, X., Jiang, S., Wang, X., and Kellner, A. W. 2017. New anatomical information of the
- wukongopterid *Kunpengopterus sinensis* Wang et al., 2010 based on a new
- specimen. *PeerJ*, **5**, e4102.
- 1001 Chu, Z., He, H., Ramezani, J., Bowring, S. A., Hu, D., Zhang, L., Zheng, X., Wang, X.,
- **Zhou, Z., Deng, C., Guo, J. 2016.** High-precision U-Pb geochronology of the Jurassic
- Yanliao Biota from Jianchang (western Liaoning Province, China): Age constraints on the rise
- of feathered dinosaurs and eutherian mammals. Geochemistry, Geophysics, Geosystems, 17
- 1005 (10), 3983-3992.
- 1006 **Dalla Vecchia, F. M. 1998.** New observations on the osteology and taxonomic status of
- 1007 Preondactylus buffarinii Wild, 1984 (Reptilia, Pterosauria). Bollettino della Società
- 1008 Paleontologica Italiana, **36**, 355–366.
- 1009 **Dalla Vecchia, F. M. 2002**. Observations on the non–pterodactyloid pterosaur Jeholopterus
- ningchengensis from the Early Cretaceous of northeastern China. *Natura Nascosta*, **24**, 8–27.
- 1011 **Dalla Vecchia, F. M. 2009.** Anatomy and systematics of the pterosaur *Carniadactylus* gen. n.
- rosenfeldi (Dalla Vecchia, 1995). Rivista Italiana di Paleontologia e stratigrafia, 115 (2),
- 1013 159–188.
- 1014 Dalla Vecchia, F. M. 2014. Triassic pterosaurs. Geological Society, London, Special
- 1015 *Publications*, **379** (1), 119–155.
- 1016 **Dalla Vecchia, F. M. 2018.** Comments on Triassic pterosaurs with a commentary on the"
- ontogenetic stages" of Kellner (2015) and the validity of Bergamodactylus wildi. Rivista
- 1018 Italiana di Paleontologia e Stratigrafia, **124** (2).
- 1019 Dalla Vecchia, F. M. 2019. Seazzadactylus venieri gen. et sp. nov., a new pterosaur (Diapsida:
- 1020 Pterosauria) from the Upper Triassic (Norian) of northeastern Italy. *PeerJ*, 7, e7363.
- 1021 Dalla Vecchia, F. M., Wild, R., Hopf, H., and Reitner, J. 2002. A crested rhamphorhynchoid
- pterosaur from the Late Triassic of Austria. Journal of Vertebrate Paleontology, 22 (1), 196–
- 1023 199.



- 1024 **Döderlein, L. 1923.** Anurognathus ammoni ein neuer Flugsaurier. Sitzungsberichte der
- Bayerischen Akademie der Wissenschaften, Mathematisch-Naturwissenschaftlichen, 1923,
- 1026 117–164
- 1027 Gao, K., and Shubin, N. H. 2012. Late Jurassic salamandroid from western Liaoning,
- 1028 China. Proceedings of the National Academy of Sciences, **109** (15), 5767–5772.
- 1029 Gao, K., Li, Q., Wei, M., Pak, H., and Pak, I. 2009. Early Cretaceous birds and pterosaurs
- from the Sinuiju Series, and geographic extension of the Jehol Biota into the Korean
- 1031 Peninsula. *J Paleontol Soc Korea*, **25** (1), 57–61.
- Goloboff, P. A., Farris, J. S., and Nixon, K. C. 2008. TNT, a free program for phylogenetic
- analysis. *Cladistics*, **24** (5), 774–786.
- Habib, M. B. 2011. Functional morphology of anurognathid pterosaurs. *In Geological Society of*
- 1035 America Abstracts with Programs 43 (1), 118.
- Holgado, B., Pêgas, R. V., Canudo, J. I., Fortuny, J., Rodrigues, T., Company, J., and
- Kellner, A. W. 2019. On a new crested pterodactyloid from the Early Cretaceous of the
- 1038 Iberian Peninsula and the radiation of the clade Anhangueria. Scientific reports, 9 (1), 1–10.
- 1039 Hone, D. W. 2020. A review of the taxonomy and palaeoecology of the Anurognathidae
- 1040 (Reptilia, Pterosauria). Acta Geologica Sinica-English Edition. In press.
- **Huang, D. 2015.** Yangliao biota and Yanshan movement (in Chinese). *Acta Palaeontologica*
- 1042 *Sinica*, **54**, 501–546.
- Huang, D. 2016. The Daohugou Biota (in Chinese). Shanghai: Shanghai Scientific & Technical
- Publishers. 332 pp.
- Huang, D. 2019. Jurassic integrative stratigraphy and timescale of China. Science China Earth
- 1046 *Sciences*, **62**, 223–255.
- Jensen, J. A., and Padian, K. 1989. Small pterosaurs and dinosaurs from the Uncompange
- fauna (Brushy Basin member, Morrison formation:? Tithonian), late Jurassic, western
- 1049 Colorado. *Journal of Paleontology*, 364–373.



- 1050 Ji, S. and Ji, Q. 1998. Discovery of a new pterosaur in Western Liaoning, China. Acta
- 1051 *Geologica Sinica* **71**, 115.
- 1052 Ji, Q., and Yuan, C. 2002. Discovery of two kinds of protofeathered pterosaurs in the Mesozoic
- Daohugou Biota in the Ningcheng region and its stratigraphic and biologic
- significances. *Geological Review*, **48** (2), 221–224.
- Jiang, S., Wang, X., Cheng, X., Costa, F. R., Huang, J., and Kellner, A. W. 2015. Short note
- on an anurognathid pterosaur with a long tail from the Upper Jurassic of China. *Historical*
- 1057 *Biology*, **27** (6), 718–722.
- 1058 Kellner, A. W.. 2003. Pterosaur phylogeny and comments on the evolutionary history of the
- group. Geological Society, London, Special Publications, 217, 105–137.
- 1060 Kellner, A. W., Wang, X., Tischlinger, H., Campos, D. A., Hone, D. W., Meng, X. 2010. The
- soft tissue of Jeholopterus (Pterosauria, Anurognathidae, Batrachognathinae) and the structure
- of the pterosaur wing membrane. *Proceedings of the Royal Society B: Biological*
- 1063 Sciences, **277** (1679), 321–329.
- Li, B., Cheng, J., Liu, M., Yang, F., Wu, Z., Du, J. 2019. Formation age and geochemical
- characteristics of the Tiaojishan Formation in the Western Liaoning Province (in Chinese).
- 1066 *Geological Review*, **65**, 63-64.
- 1067 Liu, Y., Liu, Y., and Yang, Z. 2006. U-Pb zircon age for the Daohugou Biota at Ningcheng of
- Inner Mongolia and comments on related issues. *Chinese Science Bulletin*, **51** (21), 2634-
- 1069 2644
- 1070 Liu, Y., Kuang, H., Jiang, X., Peng, N., Xu, H., Sun, H. 2012. Timing of the earliest known
- feathered dinosaurs and transitional pterosaurs older than the Jehol Biota. *Palaeogeography*,
- 1072 *Palaeoclimatology, Palaeoecology*, **323**,1–12.
- Longrich, N. R., Martill, D. M., and Andres, B. 2018. Late Maastrichtian pterosaurs from
- North Africa and mass extinction of Pterosauria at the Cretaceous–Paleogene boundary. *PLoS*
- 1075 *biology*, **16** (3), e2001663.
- 1076 Lü, J. 2009. A new non-pterodactyloid pterosaur from Qinglong County, Hebei Province of
- 1077 China. Acta Geologica Sinica-English Edition, 83 (2), 189-199.



- 1078 Lü, J., and Bo, X. 2011. A new rhamphorhynchid pterosaur (Pterosauria) from the Middle
- Jurassic Tiaojishan Formation of western Liaoning, China. Acta Geologica Sinica-English
- 1080 Edition, **85** (5), 977-983.
- 1081 Lü, J., and Hone, D. W. 2012. A new Chinese anurognathid pterosaur and the evolution of
- pterosaurian tail lengths. Acta Geologica Sinica-English Edition, **86** (6), 1317–1325.
- 1083 Lü, J., Fucha, X., Chen, J. 2010. A new scaphognathine pterosaur from the Middle Jurassic of
- western Liaoning, China. *Diqiu Xuebao(Acta Geoscientica Sinica)*, **31** (2), 263-266.
- 1085 Lü, J., Jin, X., Gao, C., Du, T., Ding, M., Sheng, Y., Wei, X. 2013. Dragons of the Skies
- 1086 (recent advances on the study of pterosaurs from China) (in Chinese). Zhejiang Science &
- 1087 Technology Press, 127.
- Lü, J., Meng, Q., Wang, B., Liu, D., Shen, C. and Zhang, Y. 2018. Short note on a new
- anurognathid pterosaur with evidence of perching behaviour from Jianchang of Liaoning
- 1090 Province, China. Geological Society, London, Special Publications, 455, 95–104.
- 1091 Lü, J., Unwin, D. M., Jin, X., Liu, Y., Ji, Q. 2009. Evidence for modular evolution in a long-
- tailed pterosaur with a pterodactyloid skull. Proceedings of the Royal Society B: Biological
- 1093 Sciences **277(1680)**: 383-389.
- 1094 **Padian, K. 1983.** Osteology and functional morphology of *Dimorphodon macronyx* (Buckland)
- 1095 (Pterosauria: Rhamphorhynchoidea) based on new material in the Yale Peabody Museum.
- 1096 *Postilla*, **189**, 1–44.
- 1097 Padian, K. 2008a. The Toarcian (Early Jurassic) pterosaur *Dorygnathus*
- 1098 Wagner, 1860. *Palaeontology*, 80, 1–64.
- 1099 **Padian, K. 2008b.** The Early Jurassic pterosaur *Campylognathoides* Strand,
- 1100 1928. *Palaeontology* 80, 65–107.
- 1101 Pêgas, R. V., Holgado, B. and Leal, M. E. C. 2019. On Targaryendraco wiedenrothi gen. nov.
- 1102 (Pterodactyloidea, Pteranodontoidea, Lanceodontia) and recognition of a new cosmopolitan
- lineage of Cretaceous toothed pterodactyloids. *Historical Biology*, **2019**, 1–15.



- 1104 **Riabinin, A. N. 1948.** Remarks on a flying reptile from the Jurassic of Kara-Tau. [In Russian.]
- 1105 Akademii Nauk,
- 1106 *Paleontological Institute, Trudy* **15**, 86–93.
- 1107 **Stecher, R. 2008.** A new Triassic pterosaur from Switzerland (Central Austroalpine, Grisons),
- 1108 Raeticodactylus filisurensis gen. et sp. nov. Swiss Journal of Geosciences, **101** (1), 185–201.
- 1109 Unwin, D. M., Lü, J., and Bakhurina, N. N. 2000. On the systematic and stratigraphic
- significance of pterosaurs from the Lower Cretaceous Yixian Formation (Jehol Group) of
- 1111 Liaoning, China. *Fossil Record*, **3** (1), 181–206.
- 1112 Unwin, D. M. 2003. On the phylogeny and evolutionary history of pterosaurs. *Geological*
- 1113 Society, London, Special Publications, 217, 139–190.
- 1114 Wang, X., Zhou, Z., Zhang, F., and Xu, X. 2002. A nearly completely articulated
- rhamphorhynchoid pterosaur with exceptionally well–preserved wing membranes and "hairs"
- from Inner Mongolia, northeast China. *Chinese Science Bulletin*, **47** (3), 226–230.
- 1117 Wang, X., Kellner, A. W., Zhou, Z., Campos, D. A., 2005. Pterosaur diversity and faunal
- turnover in Cretaceous terrestrial ecosystems in China. *Nature*, **437** (7060), 875–879.
- 1119 Wang, X., Kellner, A. W., Jiang, S., Meng, X. 2009. An unusual long-tailed pterosaur with
- elongated neck from western Liaoning of China. *Anais da Academia Brasileira de*
- 1121 *Ciências*, **81** (4), 793–812.
- 1122 Wang, X., Kellner, A. W., Jiang, S., Cheng, X., Meng, X., Rodrigues, T. 2010. New long-
- tailed pterosaurs (Wukongopteridae) from western Liaoning, China. *Anais da Academia*
- 1124 *Brasileira de Ciências*, **82** (4), 1045–1062.
- 1125 Wang, X., Kellner, A. W., Jiang, S., and Cheng, X. 2012. New toothed flying reptile from
- Asia: close similarities between early Cretaceous pterosaur faunas from China and
- 1127 Brazil. *Naturwissenschaften*, **99** (4), 249–257.
- 1128 Wellnhofer, P. 1975. Die Rhamphorhynchoidea (Pterosauria) der
- Oberjura-Plattenkalke Suddeutschlands. *Palaeontogr A.*, **148**, 1–33.
- Wellnhofer, P. 1991. The Illustrated Encyclopaedia of Pterosaurs. London, Salamander Books.



Witton, M. P. 2008. A new approach to determining pterosaur body mass and its implications 1131 for pterosaur flight. Zitteliana, 143–158. 1132 Witton, M. P. 2013. Pterosaurs: natural history, evolution, anatomy. Princeton University Press. 1133 1134 Wu, W., Zhou, C., Andres, B. 2017. The toothless pterosaur Jidapterus edentus (Pterodactyloidea: Azhdarchoidea) from the Early Cretaceous Jehol Biota and its 1135 1136 paleoecological implications. *PloS One*, **12**, e0185486. Yang, Z., Jiang, B., McNamara, M. E., Kearns, S. L., Pittman, M., Kaye, T. G., Orr, P. J., 1137 Xu, X., Benton, M. J. 2019. Pterosaur integumentary structures with complex feather-like 1138 1139 branching. *Nature ecology and evolution*, **3** (1), 24–30. Young, C. 1964. On a new pterosaurian from Sinkiang, China. Vertebrate Palasiatica 8, 221– 1140 1141 225. Zhang, H., Wang, M., Liu, X. 2008. The upper age limit of Tiaojishan Formation (western 1142 1143 Liaoning and northern Hebei area) volcanic rocks by LA-ICP-MS (in Chinese). Chinese Science Bulletin, 15, 1815-1824. 1144 1145 Zhang, Y., Chen, H. 2015. Study on the characteristics of Tiaojishan Formation (Middle Jurassic) laminar volcanic structure of Chengde Basin (in Chinese). Hebei Geology, 4, 8-10. 1146 1147 **Figures** 1148 Figure 1. Fossil provenance. Maps indicating Hebei province (China). JPM-2012-001 comes 1149 from the Mutoudeng locality. 1150 1151 Figure 2. Sinomacrops bondei tax. nov., holotype (JPM-2012-001) overview. A, photograph; and B, schematic drawing. Abbreviations: ca, caudal vertebrae; co, coracoid; cv, cervical 1152 vertebrae; d, dentary; fe, femur; fi, fibula; hu, humerus; mcIV, metacarpal IV; pip, puboischiadic 1153 plate; prap, preacetabular process of the illium; rd, radius; sca, scapula; sk, skull; ul, ulna; wp, 1154 wing phalanx. Scale bar equals 20 mm. 1155 Figure 3. Sinomacrops bondei tax. nov., skull of JPM-2012-001. A, photograph; and B, 1156 1157 schematic drawing. Light grey represents bones; dark grey represents soft tissue. Abbreviations:



- apf, anterior process of the frontal; cv, cervical vertebrae; d, dentary; f, frontal; j, jugal; la,
- lacrimal; na, nasal; pa, parietal; po, postorbital; pm, premaxilla; op, opisthotic; scr, sclerotic ring.
- 1160 Scale bar equals 10 mm.
- 1161 Figure 4. Computed-tomography images of the wings of JPM-2012-001. A, right wing; B,
- left wing. Abbreviations: d, digit; dc, deltopectoral crest; hu.ep, humeral epiphysis; mc,
- metacarpal; ph, phalanx; rd, radius; ul, ulna.
- Figure 5. Sacral region of JPM-2012-001. A, photograph; B, schematic drawing.
- Abbreviations: ac, acetabulum; ca, caudal vertebrae; fe, femur; pip, puboischiadic plate; prap,
- preacetabular process of the illium; sa, sacral vertebrae; sr, sacral rib. Scale bar equals 10 mm.
- Figure 6. Right pes of JPM-2012-001. Abbreviations: mt, metatarsal. Scale bar equals 10 mm.
- 1168 Figure 7. Phylogenetic analysis results. Strict consensus tree showing the phylogenetic
- relationships of *Sinomacrops bondei* and anurognathids. Dashed line indicates result exclusive to
- the semi-strict consensus tree.
- 1171 Figure 8. Variation in anurognathid jaw shape. Schematic drawings of anurognathid
- mandibles in ventral view. A, *Batrachognathus volans* (based on Riabinin 1948). B,
- 1173 Sinomacrops bondei. C. Jeholopterus ningchengensis (based on Yang et al. 2018). D.
- 1174 Vesperopterylus lamadongensis (based on Lü et al. 2018). Not to scale, adjusted to matching
- 1175 sizes.
- 1176 Figure 9. Schematic drawings of anurognathid humeri. A, Batrachognathus volans (based on
- 1177 Riabinin 1948). B, Sinomacrops bondei. C, Dendrorhynchoides curvidentatus (based on Ji & Ji
- 1178 1999). D, Jeholopterus ningchengensis (based on Kellner et al. 2009). E, Vesperopterylus
- 1179 lamadongensis (based on Lü et al. 2018). F, Anurognathus ammoni based on Wellnhofer (1991).
- Not to scale, adjusted to matching sizes. Abbreviations: dc, deltopectoral crest; uc, ulnar crest.
- Figure 10. Previous phylogenetic hypotheses for the position of the Anurognathidae.
- 1182 Simplified cladograms. A, from Kellner (2003). B, from Unwin (2003). C, from Dalla Vecchia
- 1183 (2019). D, from Andres *et al.* (2010, 2014). E, from Vidovic & Martill (2018). Red arrows
- indicate the Anurognathidae.

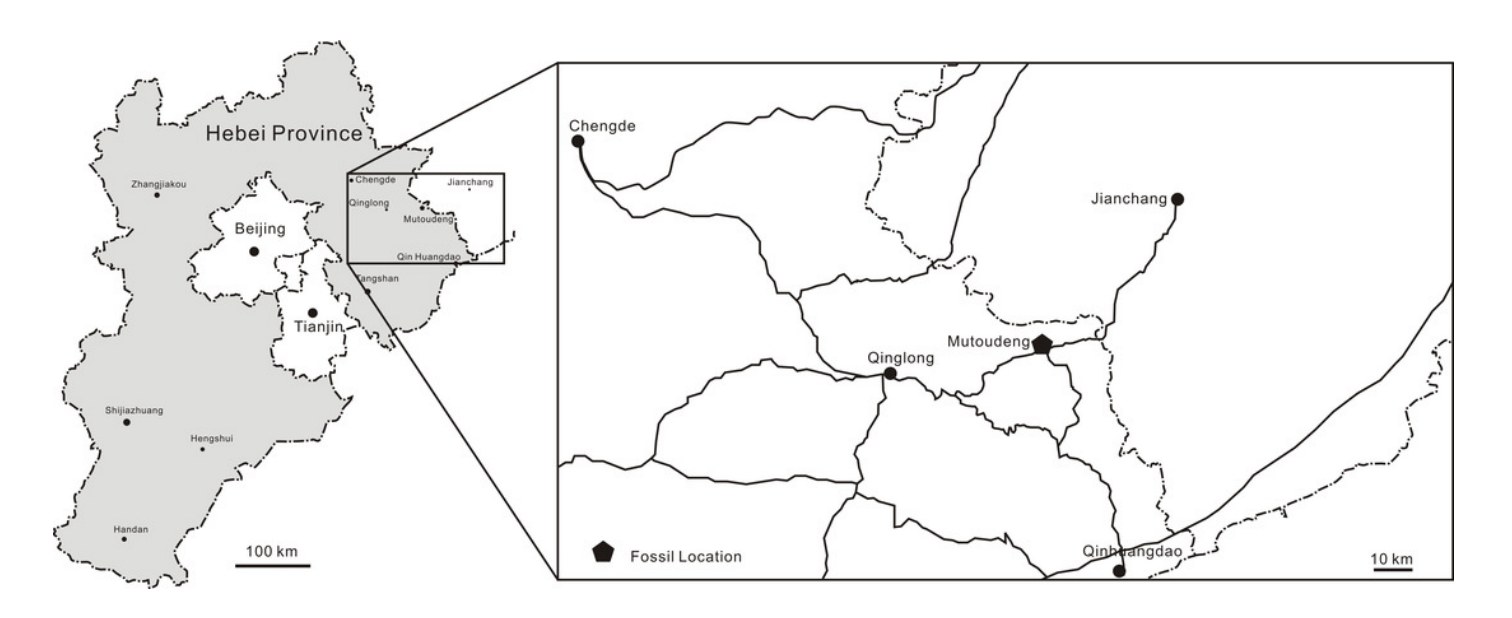


- 1185 Figure 11. Life reconstruction of Sinomacrops bondei. Paleoart courtesy of Zhao Chuang,
- 1186 reproduced with permission.



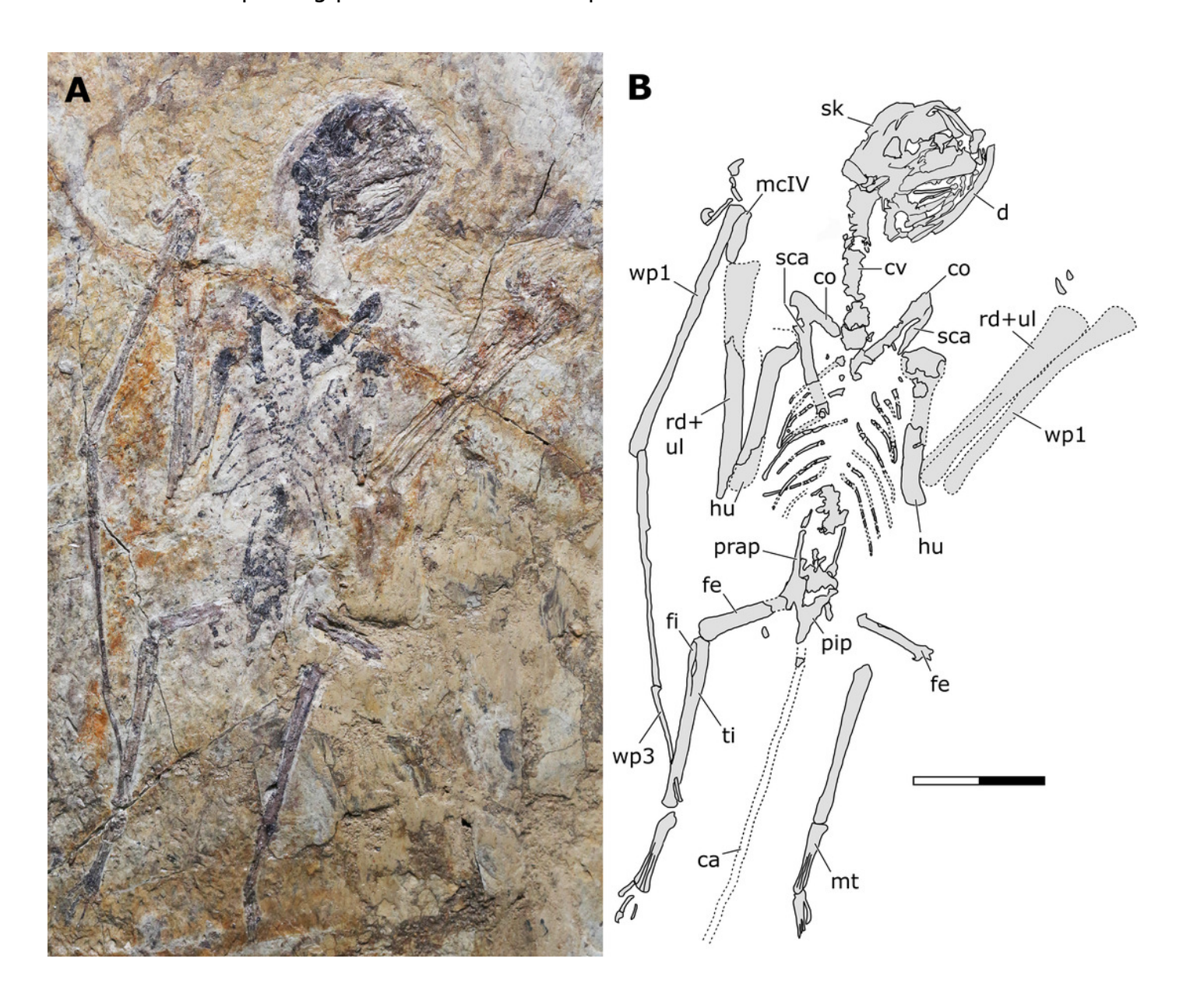
Fossil provenance.

Maps indicating Hebei province (China). JPM-2012-001 comes from the Mutoudeng locality.



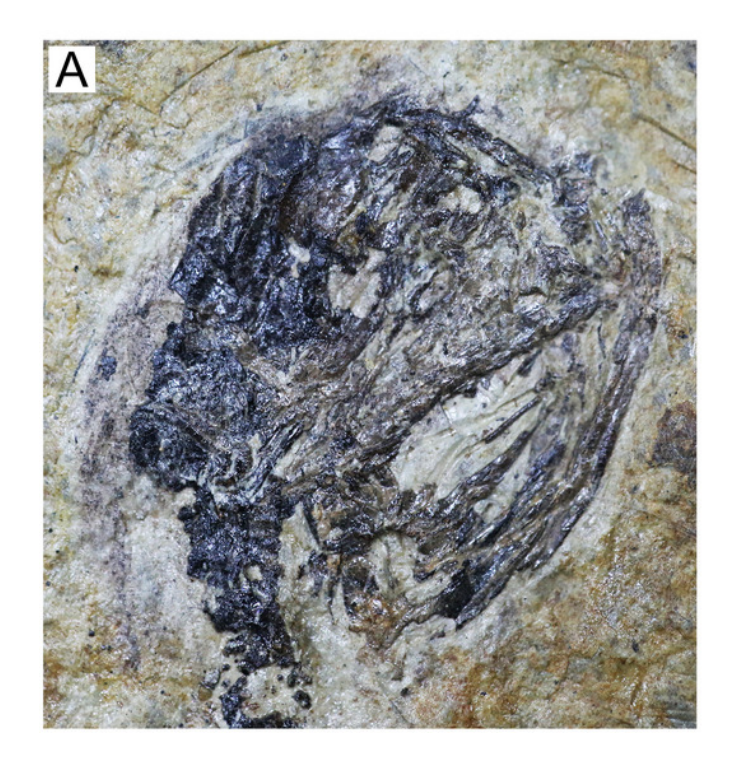
Sinomacrops bondei tax. nov., holotype (JPM-2012-001) overview.

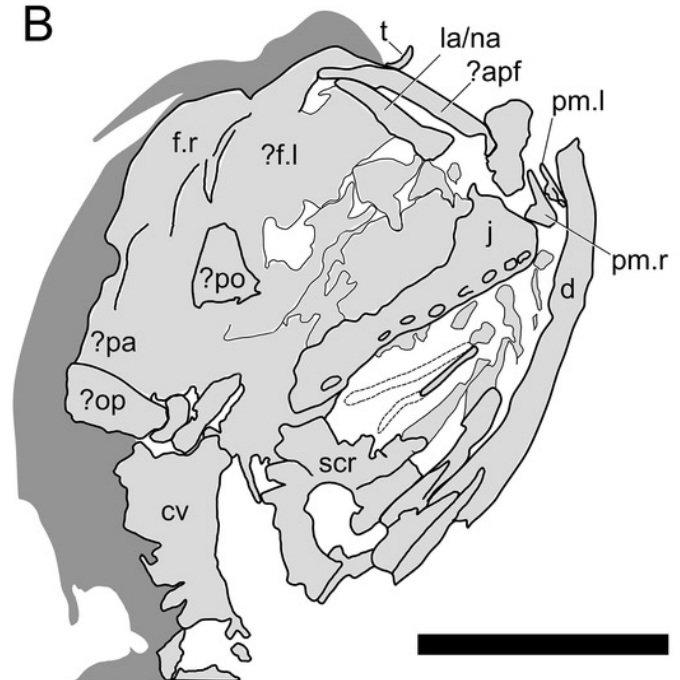
A, photograph; and B, schematic drawing. Abbreviations: ca, caudal vertebrae; co, coracoid; cv, cervical vertebrae; d, dentary; fe, femur; fi, fibula; hu, humerus; mcIV, metacarpal IV; pip, puboischiadic plate; prap, preacetabular process of the illium; rd, radius; sca, scapula; sk, skull; ul, ulna; wp, wing phalanx. Scale bar equals 20 mm.



Sinomacrops bondei tax. nov., skull of JPM-2012-001.

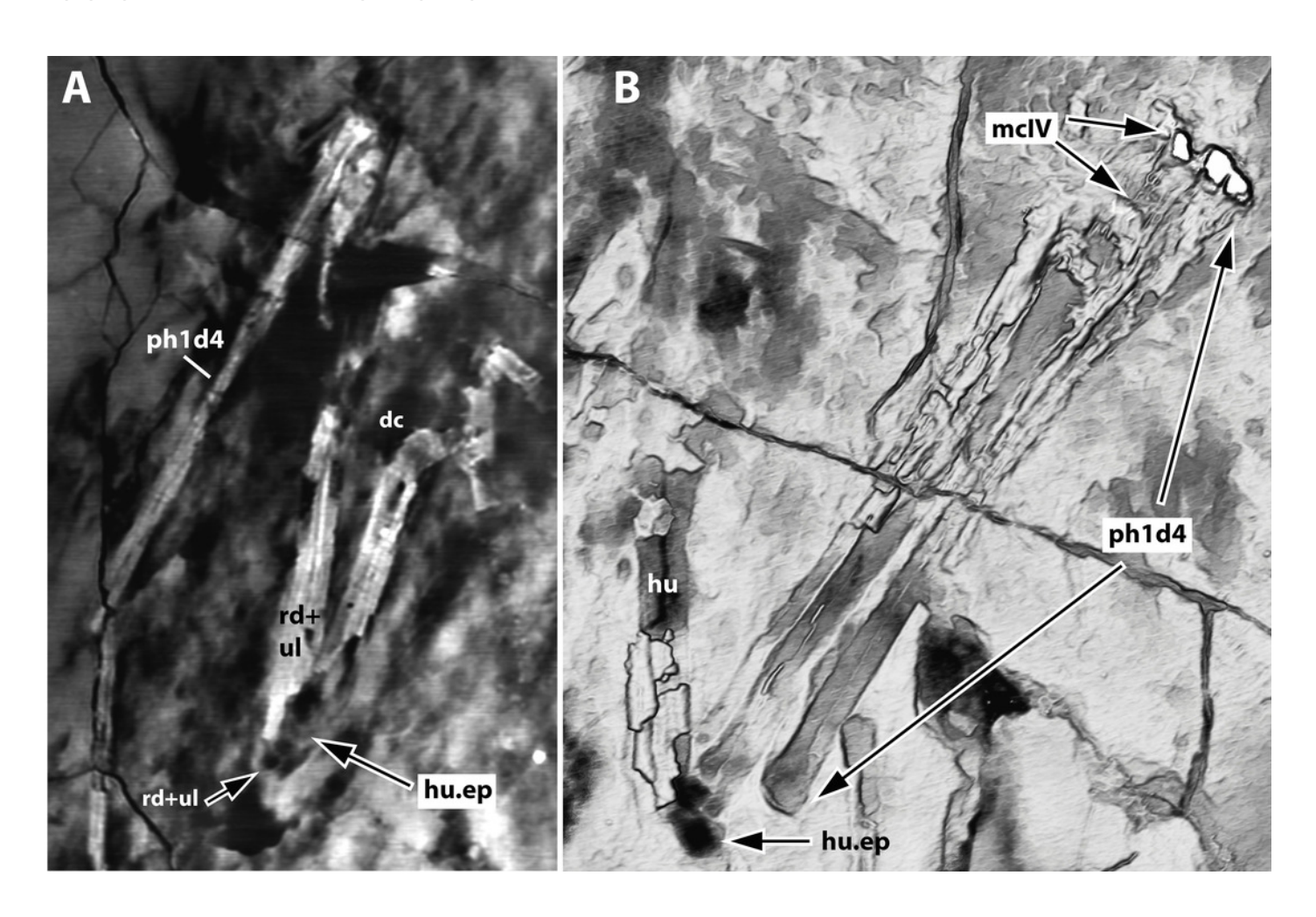
A, photograph; and B, schematic drawing. Light grey represents bones; dark grey represents soft tissue. Abbreviations: apf, anterior process of the frontal; cv, cervical vertebrae; d, dentary; f, frontal; j, jugal; la, lacrimal; na, nasal; pa, parietal; po, postorbital; pm, premaxilla; op, opisthotic; scr, sclerotic ring. Scale bar equals 10 mm.





Computed-tomography images of the wings of JPM-2012-001.

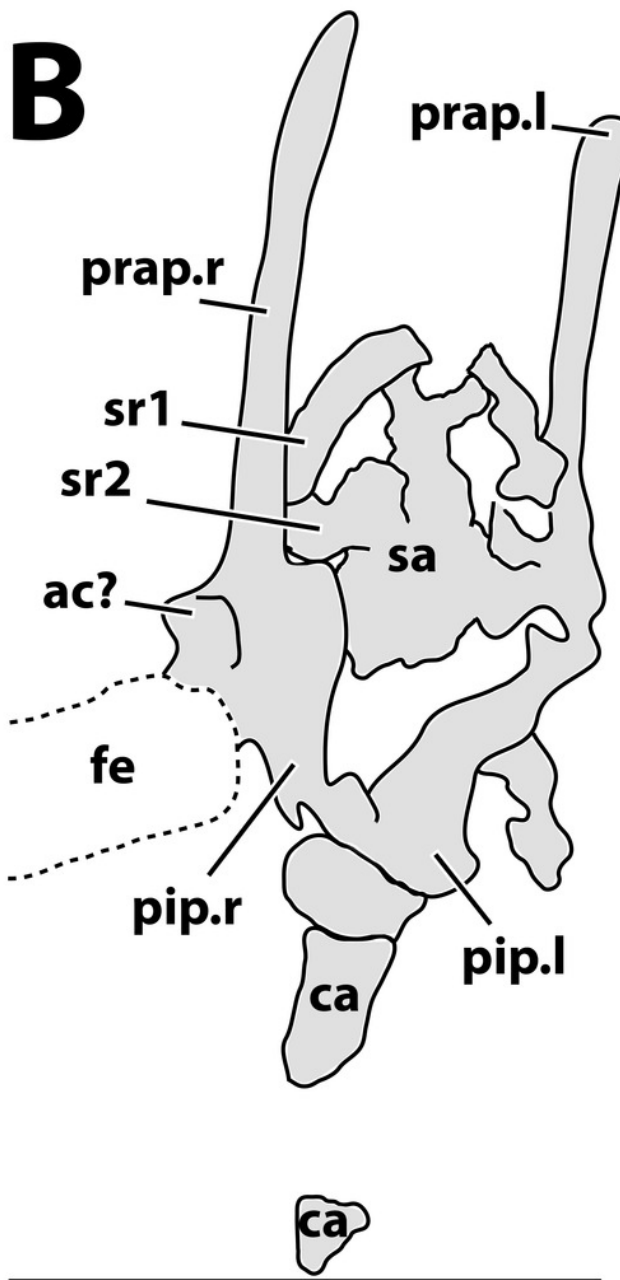
A, right wing; B, left wing. Abbreviations: d, digit; dc, deltopectoral crest; hu.ep, humeral epiphysis; mc, metacarpal; ph, phalanx; rd, radius; ul, ulna.



Sacral region of JPM-2012-001.

A, photograph; B, schematic drawing. Abbreviations: ac, acetabulum; ca, caudal vertebrae; fe, femur; pip, puboischiadic plate; prap, preacetabular process of the illium; sa, sacral vertebrae; sr, sacral rib. Scale bar equals 10 mm.

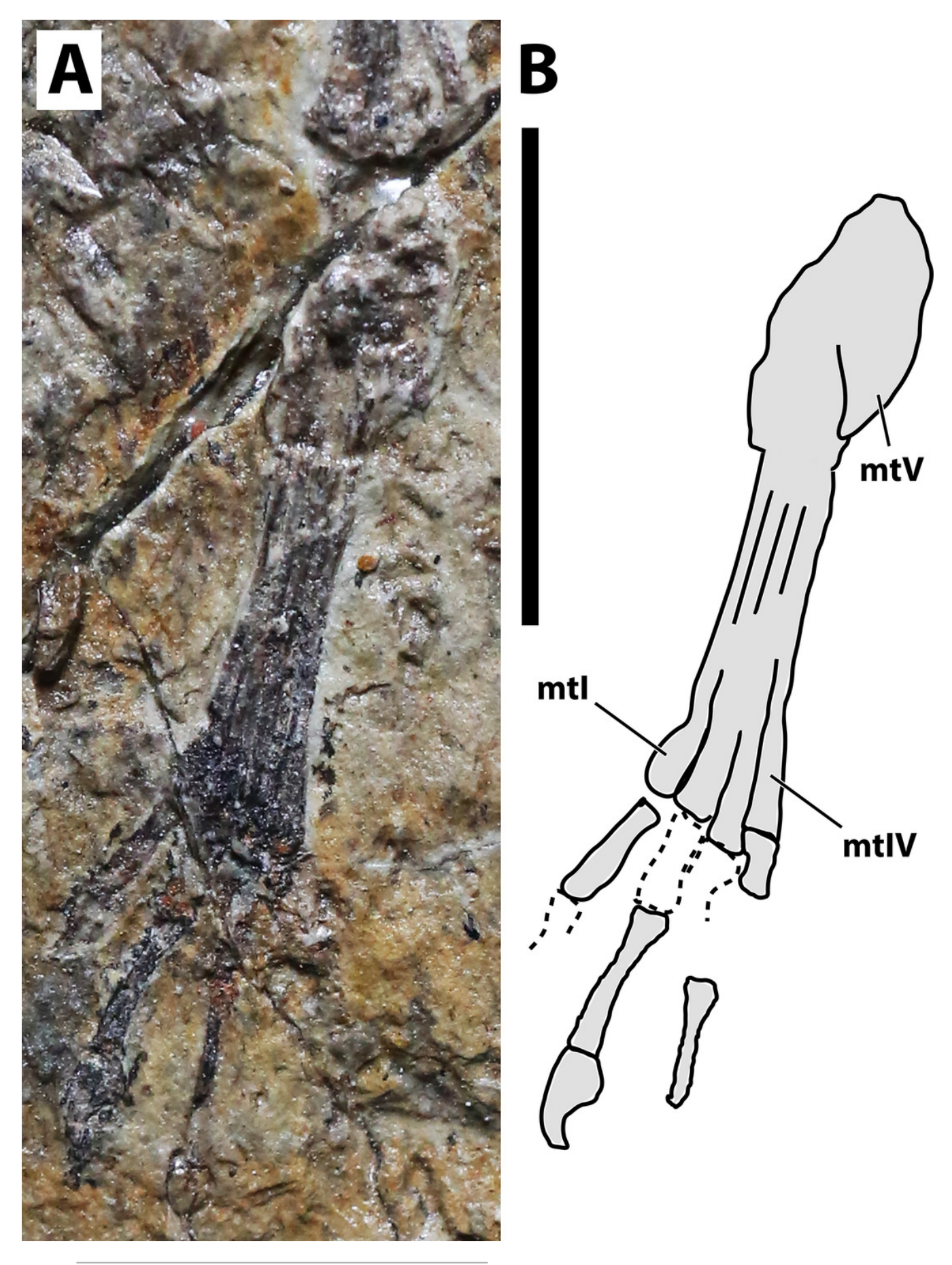






Right pes of JPM-2012-001.

Abbreviations: mt, metatarsal. Scale bar equals 10 mm.

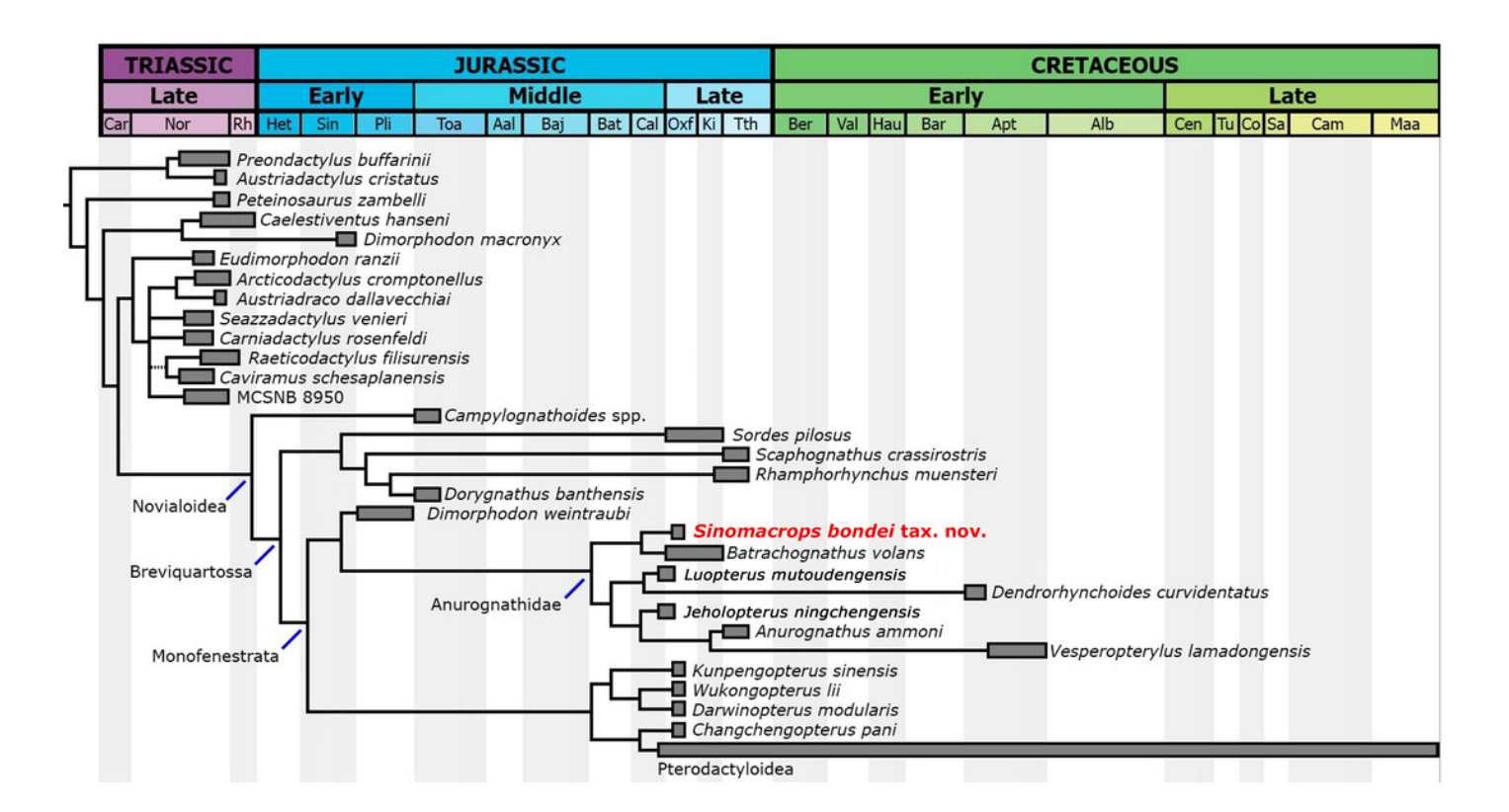


PeerJ reviewing PDF | (2020:10:53890:0:2:NEW 27 Oct 2020)



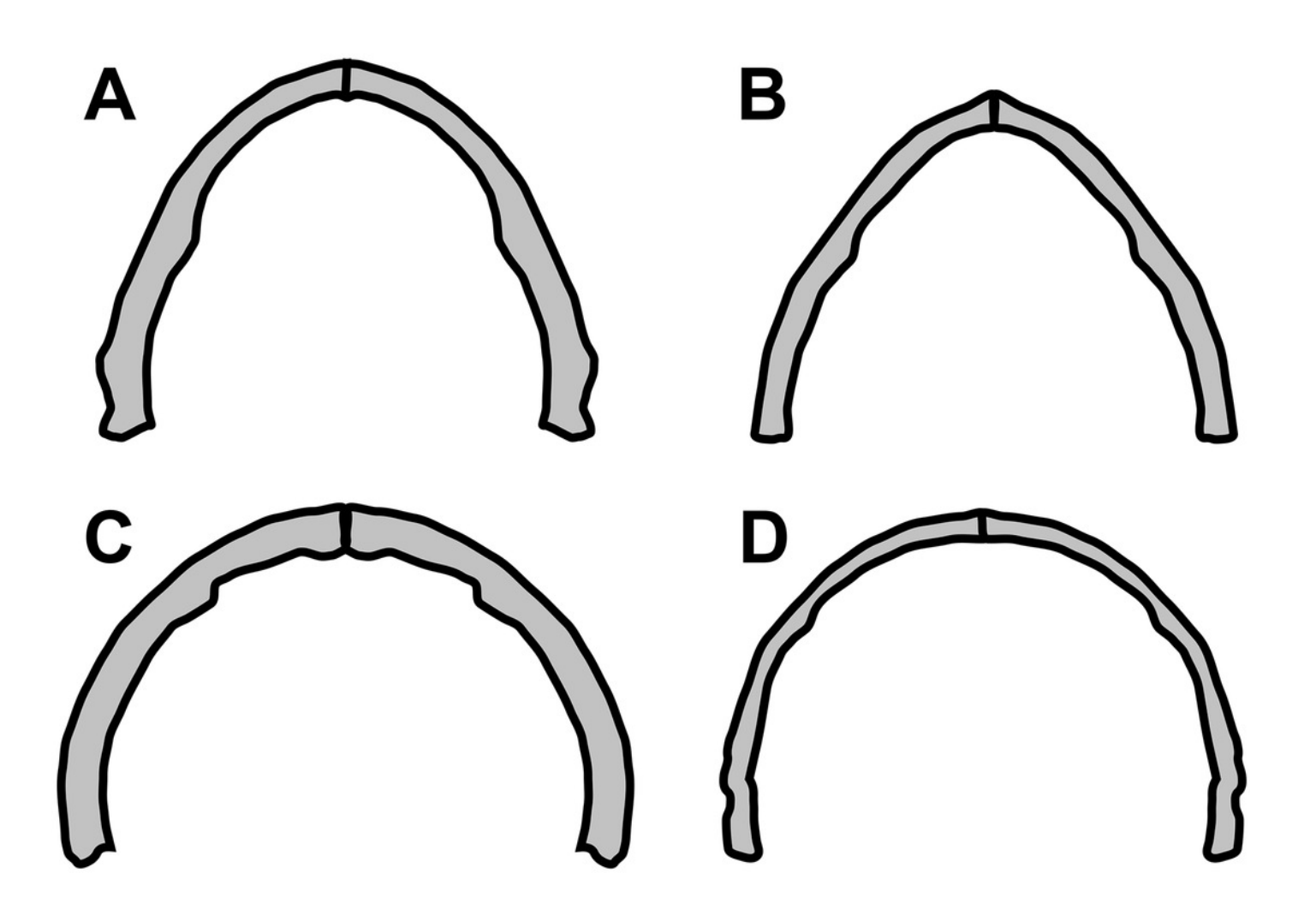
Phylogenetic analysis results.

Strict consensus tree showing the phylogenetic relationships of *Sinomacrops bondei* and anurognathids. Dashed line indicates result exclusive to the semi-strict consensus tree.



Variation in anurognathid jaw shape.

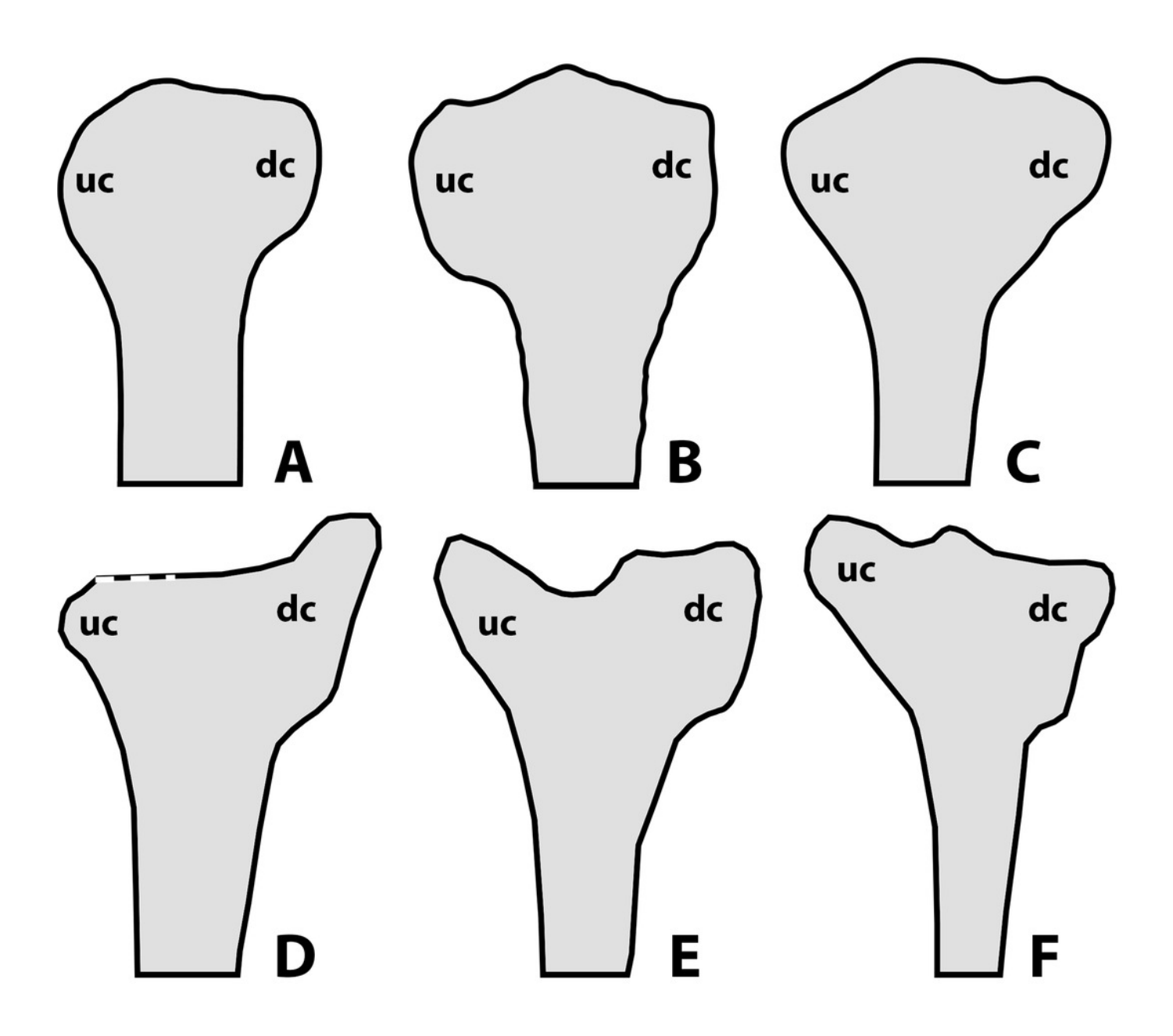
Schematic drawings of anurognathid mandibles in ventral view. A, *Batrachognathus volans* (based on Riabinin 1948). B, *Sinomacrops bondei*. C, Jeholopterus ningchengensis (based on Yang *et al.* 2018). D, *Vesperopterylus lamadongensis* (based on Lü *et al.* 2018). Not to scale, adjusted to matching sizes.





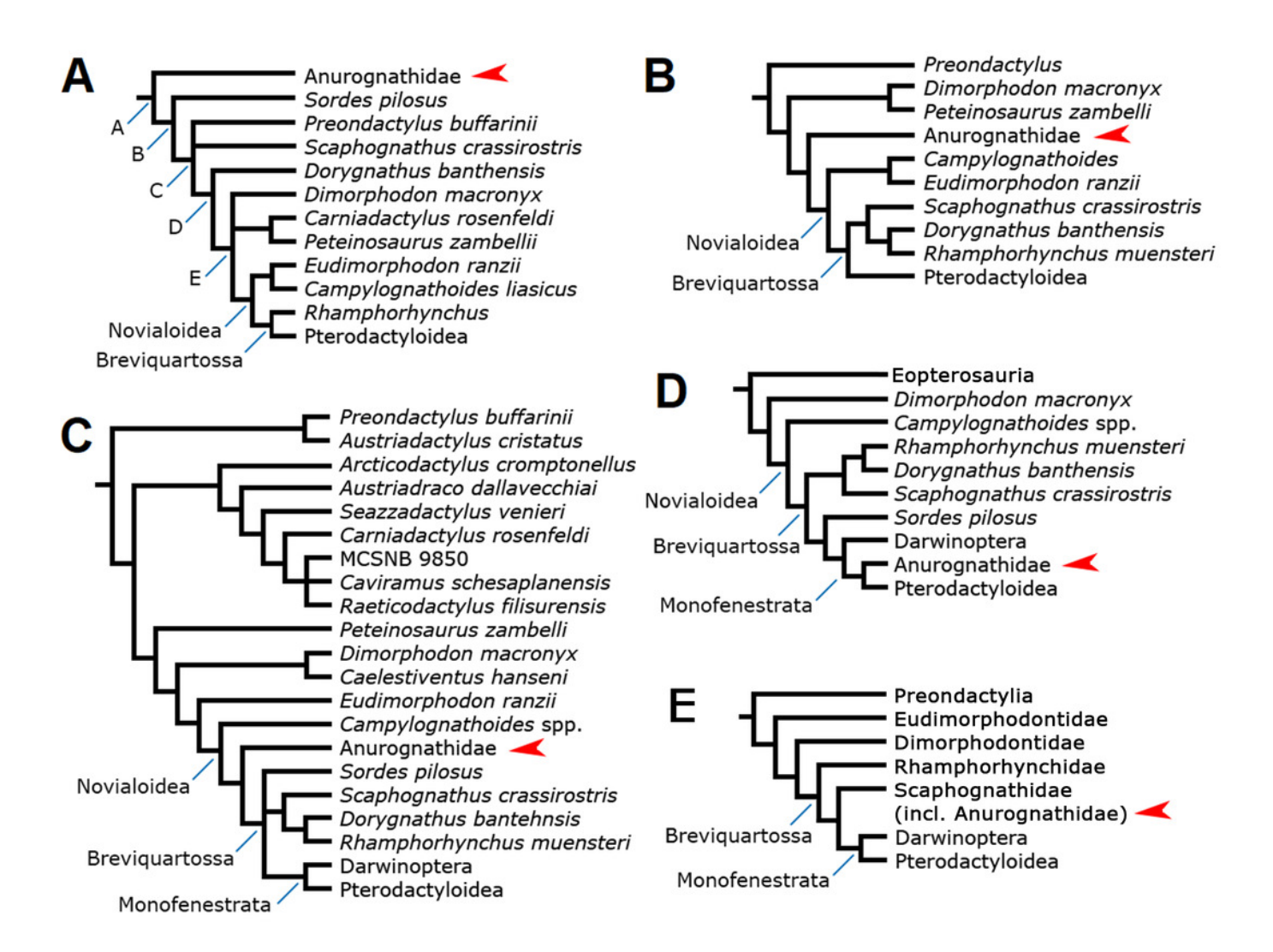
Schematic drawings of anurognathid humeri.

A, Batrachognathus volans (based on Riabinin 1948). B, Sinomacrops bondei. C, Dendrorhynchoides curvidentatus (based on Ji & Ji 1999). D, Jeholopterus ningchengensis (based on Kellner et al. 2009). E, Vesperopterylus lamadongensis (based on Lü et al. 2018). F, Anurognathus ammoni based on Wellnhofer (1991). Not to scale, adjusted to matching sizes. Abbreviations: dc, deltopectoral crest; uc, ulnar crest.



Previous phylogenetic hypotheses for the position of the Anurognathidae.

Simplified cladograms. A, from Kellner (2003). B, from Unwin (2003). C, from Dalla Vecchia (2019). D, from Andres *et al.* (2010, 2014). E, from Vidovic & Martill (2018). Red arrows indicate the Anurognathidae.





Life reconstruction of Sinomacrops bondei.

Paleoart courtesy of Zhao Chuang, reproduced with permission.



PeerJ reviewing PDF | (2020:10:53890:0:2:NEW 27 Oct 2020)



#### Table 1(on next page)

Skeletal proportions in anurognathids.

Abbreviations: caS, caudal series; co, coracoid; fe, femur; hu, humerus; mc, metacarpal; mt, metatarsal; ph, phalanx; rd, radius; sc, scapula; ti, tibia; ul, ulna. \*CaS/fe ratio for *Batrachognathus* is based on the referred specimen (Costa *et al.*, 2013; Jiang *et al.*, 2014). Measurements from *Sinomacrops bondei* were taken first-hand, data on other species was taken from the literature (Döderlein, 1923; Riabinin, 1948; Ji & Ji, 1998; Wang *et al.*, 2002; Ji & Yuan, 2002; Bennett, 2007; Lü & Hone, 2012; Jiang *et al.*, 2014; Lü *et al.*, 2018; Yang *et al.*, 2019).

Anurognathida e	hu/ mc IV	hu/fe	hu/ ul	hu+ ul/fe +ti	ul/m cIV	ul/f e	sc/co	ph1d 4/ul+ mcI V	ph1d 4/ti	ph2d4 / ph1d4	ph3d4 / ph1d4	ph3d4 / ph2d4	ph4d4 / ph1d4	fe/m cV	ti/fe	mtII I/ti	caS/f e
Anurognathus ammoni (holotype)	2.9	1.19	0.7	1.16	4.18	1.7	?	1.01	1.49	?	?	?	?	2.45	1.44	0.46	0.50
Anurognathus ammoni (referred)	3.6	1.25	0.7	1.26	5.10	1.7	?	0.95	1.44	0.77	0.44	0.56	?	2.90	1.39	0.42	?
Vesperopterylus lamadongensis	2.7	1.35	0.7	1.34	3.73	1.8	0.97	0.96	1.64	0.81	0.60	0.74	0.12	2.04	1.37	0.47	0.59
Jeholopterus ningchengensis (holotype)	3.2	1.55	0.7	1.67	4.68	2.2	1.96	0.86	1.86	0.88	0.65	0.73	0.17	2.10	1.25	0.44	?
Jeholopterus ningchengensis (CAGS IG 02- 81)	3.3	1.52	0.7 8	1.59	4.03	1.9	1.28	0.88	1.88	0.89	?	?	?	2.02	1.22	0.47	?
Dendrorhynchoi des curvidentatus	2.9 9	1.43	0.7 8	1.37	3.82	1.8	1.15	0.99	1.66	0.80	?	?	?	2.4	1.37	0.45	?
Luopterus mutoudengensis	2.4	1.28	0.6 4	1.44	3.81	2.0	1.88	0.94	1.85	0.82	0.50	0.61	0.10	1.91	1.29	0.44	0.86
IVPP V16728	?	1.43	?	?	?	?	?	?	?	?	?	?	?	?	~1.4	0.38	>1.4
NJU-57003	2.6	1.34	0.6	1.42	4.31	2.1	1.27	0.90	1.63	0.86	0.40	0.46	0.10	1.97	1.47	0.45	1.78
Sinomacrops bondei	2.8	1.76	0.5 9	1.63	4.84	2.9	1.18	0.86	1.63	0.89	0.45	0.50	?	~1.8	2.12	0.48	>1.6 9
Batrachognathu s volans	?	1.93	?	?	?	?	?	?	?	?	?	?	?	?	1.75	?	1.47

1

3

4

**Table 1. Skeletal proportions in anurognathids.** Abbreviations: caS, caudal series; co, coracoid; fe, femur; hu, humerus; mc, metacarpal; mt, metatarsal; ph, phalanx; rd, radius; sc, scapula; ti, tibia; ul, ulna. \*CaS/fe ratio for *Batrachognathus* is based on the referred specimen (Costa *et al.*, 2013; Jiang *et al.*, 2014). Measurements from *Sinomacrops bondei* were taken first-hand, data on other species was taken from the literature (Döderlein, 1923; Riabinin, 1948; Ji & Ji, 1998; Wang *et al.*, 2002; Ji & Yuan, 2002; Bennett, 2007; Lü & Hone, 2012; Jiang *et al.*, 2014; Lü *et* 

<sup>6</sup> al., 2018; Yang et al., 2019).